ROMANIAN ACADEMY
School of Advanced Studies of the Romanian Academy
Institute of Biology Bucharest

SUMMARY OF THE PhD THESIS

Identification of morphological and structural biomarkers in plants with a role in the assessment of the impact of atmospheric pollution.

PhD SUPERVISOR:
Acad. Octavian POPESCU

PhD STUDENT:
Gabriel-Mihai MARIA

2024

CONTENTS

1. CURRENT STATE OF KNOWLEDGE

1.1. ATMOSPHERIC POLLUTION

Air pollution is defined as the release into the atmosphere of gases, very fine particles or liquid aerosols, in quantities that exceed the ability of the environment to absorb, dilute, or dissipate them (Nathanson, 2020).

In the last decades, atmospheric pollution has become one of the most serious public health problems worldwide, with severe effects on the life quality of the population and environment and a major socio-economic impact.

According to the 2019 EEA (European Environment Agency) report, conducted between 2000 and 2017, pollutant emissions and their concentrations have increased globally, and in Europe, despite the attempts to reduce them, air quality remains unsatisfactory in many areas. Air pollution is currently the most important risk factor for human health and the second biggest health concern for European citizens after climate change (EEA, 2019).

Understanding the causes of atmospheric pollution is necessary to optimize actions to reduce it, how pollutants reach the atmosphere and their transformations, the effect they have over time on the chemical composition of the atmosphere and also on human health and ecosystems, on the climate and, subsequently, on society and economy. Although air pollution affects the entire population, certain groups are more vulnerable to its health effects, such as children, the elderly, pregnant women and people with pre-existing health conditions. The same EEA report from 2019 shows that almost all Europeans living in urban areas are exposed to air pollution levels that exceed the recommended air quality limits set by the World Health Organization (WHO). Their health is particularly affected by airborne particulate matter (PM), nitrogen dioxide (NO_2), and ground-level ozone (O_3), which cause the most damage (EEA, 2019).

For instance, fine particulate air pollution (PM2,5) alone was found to cause approximately 412,000 premature deaths in 41 European countries in 2016. Approximately 374,000 of these deaths occurred in the European Union. In addition to health effects and reduced life expectancy, poor air quality also causes economic losses by increasing patient care costs, decreasing agricultural and forestry production and decreasing labor productivity (EEA, 2019).

Individual exposure to various types of pollutants increases the risk of illness caused by contaminated ambient air, as toxins can reach through the respiratory tract and other target areas of the body (Samet, 2007).

1.1.1. Types of pollutants

In the last decades, the types of air pollutants as well as their concentrations have changed significantly: traditional pollutants (SO_2 and black smoke, for example) have substantially decreased in concentration, while road traffic emissions have become the main cause of poor air quality in urban areas.

The composition, variety, and concentration of these pollutants depend on the technology with which the vehicles are equipped as well as on their operating conditions. Pollutants differ from one area to another depending on the sources of pollution and are mainly dependent on road traffic emissions because vehicles with internal combustion engines use petroleum and diesel-based fuels. The most important phytotoxic pollutants associated with road transport are nitrogen monoxide (NO) and nitrogen dioxide (NO_2). Traces of other nitrogen-containing compounds such as nitrous acid (HONO), nitrous oxide (N_2O), and ammonia (NH_3) may also be present in vehicle exhaust (Honour *et al*., 2009).

Numerous studies have been carried out over the last decades on how atmospheric pollutants change parameters such as physical structure, chemical composition and how gas exchange and ions are regulated by the foliar surface of the leaf, these being considered markers of stress caused by atmospheric pollution in industrial areas. Gaseous pollutants (entering through the stomatal ostiole) and ions in aqueous solutions, once they penetrate the leaf, can produce changes in metabolic processes and affect its surface by altering wax biosynthesis (Cape, 1994).

The main atmospheric pollutants as well as their mode of action on leaf surfaces:

- **Ozone**, a strong oxidant whose presence affects metabolic processes; it penetrates inside the plant through the stomata, but also through diffusion at the cuticle level (Matyssek *et al*., 1995).
- **Sulfur dioxide (SO_2)**, can affect the plant's metabolic processes and influence the biosynthesis of leaf surface components; short-term exposures to high concentrations of SO_2, as well as long-term exposures to low amounts of SO_2, can lead to the accumulation of SO_2 in the needle leaves of conifers and can produce harmful effects

on trees, including during the winter, when the physiological activity of the trees is low (Manninen and Huttunen, 1995).

- **Nitrogen oxides (NO and NO_2)** can directly react with cuticular structures following long-term exposure to high concentrations and can disrupt metabolic processes following foliar absorption (Cape, 1994).
- **Ammonia** can disrupt some metabolic effects and therefore the development of the leaf surface, but without a considerable direct effect (Cape, 1994).
- **Airborne particles PM** (dust or soot) or particles suspended in water droplets do not cause significant adverse effects but may accumulate to the point where stomata may become blocked or light may no longer reach the leaf surface. They can however affect the integrity of the leaf surface directly by abrasion, by the leaves touching each other, or by particles carried by the movements of air masses (Cape, 1994).

Compared to most gaseous or aqueous pollutants, only organic molecules, acid solutions, and nitrogen oxides can directly affect leaf surfaces (Cape, 1994).

1.1.2. The effect of pollution on vegetation

The presence of pollutants in the form of airborne particles in urban areas induces changes at the morphological, biochemical and physiological level in plants, and also their adaptation response to limit stress and maximize the use of internal and external resources (Rai, 2016). Following the interaction between plants and different types of pollutants, physiological, ultrastructural and biochemical changes were observed at the foliar level of plants used as indicators of atmospheric pollution (Thawale *et al*., 2011).

Several biotic and abiotic stress factors can cause structural changes at the foliar level which manifests in the appearance of macroscopic symptoms such as:

- *Premature aging* can be defined as a maturation process of some organs during which fully developed and functional tissues undergo physiological and structural changes at a progressive rate and a decreased vitality of these tissues (Günthardt-Goerg and Vollenweider, 2007).
- *Ontological senescence* is a degenerative process that takes place in the last stage of development of the cells or organs and is characterized by the change of the colour of the tree crown (yellow - occurs following the degradation of chlorophyll, red - *de novo* synthesis of anthocyanins prior to the degradation of chlorophyll, brown - occurs due to the oxidation of cellular components, black –

results from the induction of phenoloxidases following the decompartmentalization of cells) from temperate zones and the characteristic yellowing of those conifers.

- *Accelerated cellular senescence* occurs before autumn in younger leaves.
- *Accidental or programmed cell death* results from mechanical damage that can be caused by weather phenomena (hail, frost, etc.) or exposure to high concentrations of chemicals and toxic pollutants.
- *The hypersensitive response* is a process that occurs following the interaction between the plant and a pathogen and is a defence system of the plant against microbial infections. The purpose of this response is to reduce the risk of the spread and development of pathogens in healthy tissues (Heath, 2000).
- *Oxidative stress.* Accumulation of reactive oxygen species (ROS) causes oxidative stress and can lead to lipid peroxidation, protein inactivation, and DNA strand breaks (Bartosz, 1997).

1.1.2.1. Impact of heavy metal pollution on vegetation

The term "heavy metals" refers to any metallic element that has a relatively high density and has a toxic effect even in low concentrations. They belong to the group of metals and metalloids with an atomic density greater than 4 g/cm3 and include: lead (Pb), cadmium (Cd), nickel (Ni), cobalt (Co), iron (Fe), zinc (Zn), chromium (Cr), arsenic (As), silver (Ag), as well as the platinum metals (ruthenium (Ru), rhodium (Rh), palladium (Pd), osmium (Os), iridium (Ir) and platinum (Pt) (Gill, 2014). Heavy metals (Pb, Zn, Cr, and Cd) from incomplete burn of fuels as well as from industrial activities are released into the atmosphere in the form of particles of variable sizes. Plants can be used successfully as biomonitors of atmospheric pollution, studies show that an increase in heavy metal amounts, especially Pb resulting from the burning of fossil fuels and peat for home heating, causes visible effects in the surrounding vegetation (Martin *et al*., 2015).

ORIGINAL CONTRIBUTIONS

2. THE AIM OF THE STUDY

The general aim of the thesis is to propose new morphological and structural biomarkers in plants that can be used as indicators of atmospheric pollution in urban areas.

Thus, we initiated a study in which micromorphological characteristics and anatomical changes developed in the leaves of the *Pinus nigra* species, collected from several areas in Bucharest were highlighted. Both the plant material collected from the 21 different points (15 intersections and heavily trafficked roads, a less polluted area, Câmpina, and 5 points inside the Alexandru Ioan Cuza park), as well as the dust deposited on the leaves and on the walls of the exhaust pipes of automobiles, were analysed using optical microscopy, electron microscopy (SEM and SEM-EDX) and X-ray fluorescence spectrometry. Through these investigations, several objectives were pursued:

- Highlighting some morphological, micromorphological, and structural changes of *Pinus nigra* needles exposed to pollution during histological investigations and optical microscopy techniques, by comparison with samples collected from non-polluted areas.
- Observation of the deposition of various types of particulate matter on leaf surfaces using SEM electron microscopy.
- Elemental analysis of particulate deposits using X-ray fluorescence spectrometry.
- Characterization and classification of various types of airborne particles in terms of morphology and elemental composition using SEM and EDX (Energy-Dispersive X-ray) electron microscopy.

3. MATERIALS AND METHODS

3.1. BIOLOGICAL MATERIAL

The species from which the samples of biological material were collected for the identification of structural and morphological biomarkers was *Pinus nigra* J. F. Arnold. This species was selected because it presents a series of characteristics that recommend it as excellent study material for the identification of biomarkers of atmospheric pollution: it have sempervirescent leaves, which persist between 4 and 7 years and allows physiological changes to be expressed phenotypically; it is a drought and frost - resistant species that has adapted very well to the conditions of climate change; it is a species often found in the urban environment being cultivated in parks, along road arteries, gardens or various green spaces.

3.2. ANALYSIS OF LEAF SURFACES

3.2.1. The collection of plant material

The samples used in the analysis were represented by needle leaves of the species *Pinus nigra*. The establishment of the collection points of plant material samples was based

on the identification of some polluted areas within the Municipality of Bucharest with intense road traffic (intersections and main road arteries) where the species of interest could be identified and from an area considered to have the cleanest air in Romania, the city of Câmpina (control area), Prahova County.

The plant material was collected from a height of approximately 150-200 cm, this being considered the height of breathable air, according to the "Guide for the use of species in biomonitoring programs" (Ștefănuț *et al*., 2017).

The geographical coordinates of the collection points of the plant material used in our investigation are presented in Table 3.1.

Table 3.1. The geographical coordinates of the collection points of the plant material.

Sites	Geographic coordinates	Adress of the collection points
P1	44°27'05.9"N 26°02'45.9"E	Șos. Virtuții
P2	44°26'05.4"N 25°59'07.0"E	Bd. Iuliu Maniu
P3	44°24'04.3"N 26°03'09.1"E	Intrarea Ghimeș
P4	44°24'15.1"N 26°05'46.9"E	Bd. Pieptănari
P5	44°23'36.4"N 26°07'20.2"E	Șos. Olteniței
P6	44°25'34.2"N 26°07'04.8"E	Bd. Unirii
P7	44°25'39.9"N 26°06'12.9"E	Piața Unirii/Parc Unirii
P8	44°26'13.0"N 26°06'07.3"E	Bd. Nicolae Bălcescu
P9	44°27'09.8"N 26°05'11.1"E	Piața Victoriei/Cotroceni
P10	44°26'29.2"N 26°08'01.5"E	Piața Ianculului
Control Sample Câmpina	45°08'29.3"N 25°46'38.6"E	Str. Zăpodie
Control Sample Suceava	47°40'25.6"N 25°11'38.6"E	Moldova-Sulița

3.2.2. Preparation of material for optical microscopy analysis (stereomicroscopy)

The material collected from the field was analysed within 24 hours after collection to avoid secondary contamination with fungi and/or bacteria. For the stereomicroscope studies, the samples were not processed or fixed because the aim was to observe as unaltered

as possible the amount of coverage with deposits. Also, the plant material was handled with utmost caution to avoid the loss of deposits.

3.2.3. Preparation of plant material for fluctuating asymmetry analysis AF

Plant material collected from the field consisting of 100 pairs of 2-year-old needle leaves was analysed no later than 48 hours after collection and stored in a refrigerator at +4°C.

The samples were collected from 10 points within the City of Bucharest, respectively 5 points from areas free from pollution sources (samples P1, P2, P3, P4 and P5 from Alexandru Ioan Cuza Park, I.O.R) and 5 points from areas with heavy road traffic, samples P6 (Bd. Camil Ressu), P7, P8 (Bd. Mihai Bravu) and P9, P10 (Piata Iancului intersection). For the analysis of fluctuating asymmetry and general morphology, two parameters, namely the length (mm) and weight (g) of each pine needle in each pair of needles were followed.

3.2.4. Sample preparation for Scanning Electron Microscopy investigations (SEM)

For scanning electron microscopy (SEM) investigations, pine needles were cut into fragments approximately 2–3 cm long from their tip, middle, and base and mounted on aluminum electron microscope supports using electroconductive double-sided adhesive tape as well as the electroconductive paste with Ag powder so that both surfaces of the leaves, adaxially and abaxially, can be studied.

To be able to compare the results obtained from the electron microscopy analyses regarding the deposition of airborne particles on the surfaces of pine leaves, samples were also collected from the inside of the exhaust pipes of some vehicles with internal combustion engines that use both diesel and gasoline.

3.3. STRUCTURAL ANALYSIS OF LEAF FOILS

3.3.1. Samples fixation

To observe the layer of deposits on the surface of the epidermis, the plant material samples were not washed or cleaned and were handled as little as possible. Twenty-four hours after collection, samples were placed in vials containing a 1:3 volumetric mixture of glacial acetic acid and 95% ethyl alcohol. Samples were fixed in this mixture for a minimum of 12 hours before sectioning.

3.3.2. Sample sectioning

The samples subjected to sectioning consisted of fragments with a length of approximately 1 cm taken from the apex area, from the middle area, and from the base of acicular leaves. Leaf fragments were sectioned using the botanical razor and Euromex MT.500 manual microtome. Sections were made transversely and had thicknesses between 15 and 20 μm. To increase the accuracy of the observations, both fresh material samples and fixed samples were sectioned. Samples of fresh material were sectioned after a maximum of 24 hours from sampling. Transverse sections were also performed using the Histo-Line MC4000 cryotome from the Histology laboratory of the Department of Developmental Biology.

Fresh fragments of pine needles with a length of approximately 8 mm were sectioned with the help of a scalpel and placed in a cryoprotectant solution (CRYO-M-BED Embedding Compound) for 24 hours to facilitate the absorption of the solution as deeply as possible into the tissue plant. After treatment, the samples were placed in pyramid-shaped silicone molds filled with the same cryoprotectant solution and left for 30 min in the freezing chamber of the MC4000 cryotome at –20°C. After complete freezing, the samples were mounted on the aluminum support of the cryotome and cross-sections with a thickness of approximately 10-15 μm (at an angle of 10°) were made, both from the apex, the middle and from the base areas of acicular leaves, after which they were mounted on glass slides and examined with an optical microscope.

3.3.3. Sample analysis

To preserve as much as possible the cellular contents, the sections were not cleared. Also, to detect the presence of tannins in the structures, the sections were not stained.

For the visualization of the structures, temporary microscopic preparations were made by immobilizing the sections between the coverslip and the coverslip in a drop of distilled water. Sections were analysed using a Nikon Eclipse E200 microscope. Images were captured using a Nikon Coolpix 5400 digital camera attached to the microscope.

3.4. QUALITATIVE AND QUANTITATIVE ANALYSIS OF DEPOSITIONS

3.4.1. Elemental analysis using energy dispersive X-ray spectroscopy (EDX)

The studied samples consisted of both the deposits on the leaf surface of the material collected from the areas mentioned in Chapter *3.2.1 Collection of plant material* (Table 3.1.), and in the ash collected from the inside of the exhaust pipes of some diesel or gasoline

vehicles. SEM-EDX investigations followed the same sample preparation protocol as previously described in the case of SEM investigations (*3.2.3. Sample preparation for Scanning Electron Microscopy (SEM) analyses*), respectively the pine needles were cut in 2-3 cm long fragments from both their tip, middle and base and mounted on aluminium electron microscope mounts using electroconductive double-adhesive tapes and electroconductive paste with silver powder. Both qualitative and quantitative evaluations of the elements identified in the studied samples were made, and for the quantification of the elements, EDX spectrograms were recorded in which both the mass percentage and the atomic percentage of each identified element are displayed in the spectrum.

3.4.2. Elemental analysis using X-ray fluorescence spectrometry (XRF)

The total metal content was measured with Rigaku ZSX100e X-ray fluorescence spectrometer. To distinguish airborne particles deposited on leaf surfaces from those accumulated within tissues, both washed and unwashed pine needles were analysed. Both the washed and unwashed samples were oven-dried at a temperature of 60°C until the dry sample weight stabilized and ground to a fine powder. The preparation of plant samples in the form of powder was carried out in an atmosphere of He of 99.99% purity. 5 g of powder obtained from pine needles were placed in special cylindrical containers with a diameter of 30 mm (cat. No. CH1530) covered on both sides with Rigaku polypropylene film with a thickness of 6 μm (cat. No. 3399G003) and fixed with container sealing rings. The results were generated in percentages of element oxides detected in plant material powder (Young et al., 2016). The final results were expressed in mg of airborne particulate metals deposited per kg of dry material according to the formula:

$$PMD = M_{uw} - M_w \qquad (1)$$

PMD = the metal content of airborne particulate deposition;

M_{uw} = the metal content of unwashed samples;

M_w = the metal content of the washed samples.

3.4.3. Statistical analysis methods

3.4.3.1. Descriptive statistics

The statistical analyses applied for the interpretation of the results were carried out with the help of the XLSTAT Pro software program (Xlstat Add in, 2013).

Descriptive statistics along with Boxplot diagrams were used to organize and summarize the obtained data set, thus providing a comprehensive picture of the distribution, variability as well as extreme values present. Also, the selected methods allow us to compare different data sets to identify their similarities or differences. Descriptive statistics processing was done on non-logarithmic data to highlight the distribution of data collected in the field and to understand trends according to the tested criteria.

3.4.3.2. The Fisher test

Before using parametric analyses such as Fisher's Test of variances, the data were tested for normal distribution or not. For this purpose, the *Shapiro-Wilk* normality test was applied.

The Fisher F test is a statistical method used to test the differences (variability) between two different samples (two sets of data). In the case of our study, comparing the variance between two sets of data: the weight of the pine needles on the right side compared to the weight of the pine needles on the left side. The *two-tailed* Fisher-test tests differences in both directions between the variants of the two groups.

The principle of the method is based on the formulation of statistical hypotheses:
- null hypothesis (H0) - The variances of the two populations are equal;
- alternative hypothesis (H1) - The variances of the two populations are different.

The result is obtained by dividing the variance of the larger sample by the variance of the smaller sample (DuToit *et. al*, 2012).

4. RESULTS AND DISCUSSION

4.1. CHANGES IN THE LEAF MORPHOLOGY

4.1.1. The results of the measurements of some morphological parameters of *Pinus nigra* needles from areas with different degrees of atmospheric pollution

The results of the measurements of the morphological parameters of the pairs of Pinus nigra needles indicate that the plant material samples collected from areas with heavy road traffic (P6, P7, P8, P9, P10), compared to the samples collected from trees from less exposed areas urban pollution and with superior nutrition and hydration conditions (P1, P2, P3, P4, P5), present greater deviations from perfect symmetry from the point of view of the investigated parameters, namely the weight and length of the pairs of needles.

The most visible indicator of the fluctuating asymmetry FA is given by the difference between the lengths of the pairs of needles (the difference between the left and the right needle in the pair of needles in a sheath), the parameter with the highest value has been observed in samples P6 (Bd. Camil Ressu) and P7 (Bd. Mihai Bravu), and the lowest value in samples P1 and P3 (Parc Alexandru Ioan Cuza) and P10 (Piața Iancului).

The second parameter monitored to determine FA, namely the ratio between the weight of the left needle and the weight of the right needle in each pair of needles in a sheath, also indicated the greatest difference in the material collected from the Bd. Mihai Bravu area (P7 = 0,0212 g), respectively Piața Iancului (P9 = 0,0220 g). Under normal environmental conditions, the weight differences between the needle on the left side and the one on the right side are minimal, thus, weighing the needles can be considered a useful method in determining the anthropogenic impact on the environment (Mammadova, 2009).

Table 4.1. The results of the measurements of some morphological parameters of *P. nigra* needles from areas with different degrees of atmospheric pollution.

SAMPLE	SUM LEFT NEEDLE LENGTHS (MM)	SUM RIGHT NEEDLE LENGTHS (MM)	AVERAGE RATIO BETWEEN LEFT AND RIGHT NEEDLE LENGTH (MM)	AVERAGE WEIGHT LEFT NEEDLE (WASHED AND DRY)(g)	AVERAGE WEIGHT STRAIGHT NEEDLE (WASHED AND DRY) (g)	AVERAGE WEIGHT RATIO BETWEEN LEFT AND RIGHT NEEDLE(g)
P1	1413,3	1414,3	1	0,8286	0,8155	0,0131
P2	1515,7	1513,2	2,5	0,7615	0,7572	0,0043
P3	1520,2	1519,2	1	0,8006	0,7833	0,0173
P4	1379,2	1381,2	2	0,6846	0,6861	0,0015
P5	734,1	733	1,1	0,7828	0,772	0,0108
P6	1442,5	1445,5	3	0,5566	0,5617	0,0051
P7	1264	1260,2	3,8	0,7081	0,6869	0,0212
P8	1790,2	1788,5	1,7	0,8601	0,8442	0,0159
P9	1577,7	1576,6	1,1	0,6908	0,6688	0,0220
P10	1251,8	1252,1	0,3	0,6154	0,6287	0,0133

4.1.2. Descriptive analysis of Data

The results of our study indicated some differences in the traits of trees in traffic areas compared to those in park areas.

Needle sizes

The analysis of the characteristics of the dimensions of the needles in the freshly washed samples from the two types of areas revealed higher values of the needles (left needles –146,524 mm; right needles –146,458 mm) from the areas with road traffic compared to those in the park (left needles –131,250 mm; right needles – 131,218 mm). In high-traffic areas, the minimums and maximums of the needles were higher than those in the park areas, while the standard deviation showed a greater spread of data in park areas. These explain the fact that in the points inside the park, the needles showed a greater variability of their sizes.

Table 4.3. Descriptive statistics of needle sizes in the study areas.

	Park		**Road Traffic**	
Statistic	**L-PS (mm)**	**R-PS (mm)**	**L-PS (mm)**	**R-PS (mm)**
Minimum	61,000	61,000	115,800	115,500
Maximum	173,000	173,000	241,000	239,000
Average	131,250	131,218	146,524	146,458
Standard Deviation (n-1)	32,214	32,247	24,201	24,158

Abnormal values (outliers) were recorded in areas of the park, values that were much lower than the normal data range. These, for both types of needles in the clean area, pulled the averages ("+") down, thus being observed below the median.

In traffic areas, the diagrams showed similarity in terms of data spread, and in both groups, the presence of extreme values was noted which in the diagrams were also signaled as maximum values. Mean and median values were not close to the center of the distribution, indicating that the data had a slightly skewed distribution.

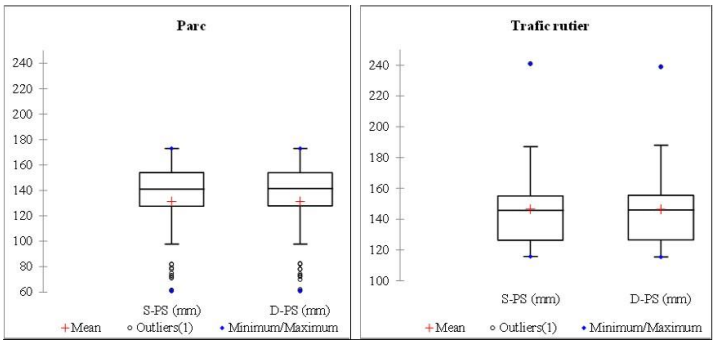

Figure 4.1. Boxplot diagram regarding the descriptive statistics of the dimensions (mm) of the needles in the study areas.

Descriptive statistics on the weight of fresh samples with deposits

The weight of needles collected from the park (fresh with deposits) from the left and right sides of the sheath showed lower minimum values (0,065 – 0,062 g) compared to those from road traffic areas (0,073 – 0,072 g). The peak values also showed that there were higher peaks in the traffic areas compared to the park areas. These were also reflected in the recorded averages that characterized these areas, which suggests that the traffic areas were characterized by slightly higher weight values (Table 4.4.). The data obtained from the park samples were more varied compared to those from the traffic areas. Even though the needle weight values collected from the park were lower, a variability of needle types was identified in this area.

Table 4.4. Descriptive statistics of weight (g) of fresh needles with deposits.

	Park		Traffic areas	
Statistic	**L-PD (g)**	**R-PD (g)**	**L-PD (g)**	**R-PD (g)**
Minimum	0,065	0,062	0,073	0,072
Maximum	0,211	0,201	0,235	0,241
Average	0,134	0,132	0,137	0,136
Standard deviation (n-1)	0,035	0,033	0,030	0,028

Road traffic areas were characterized by extreme values of needle weight, meaning that there were identified areas that significantly changed the characteristics of the samples. While the means ("+") in the park area were close to the medians, indicating a symmetry in the distribution of values for both L–PD and R–PD, in the traffic areas the means were above

the medians indicating the fact that the weighting of higher weights, such as the presence of extreme values (outliers) had an impact on the data distribution.

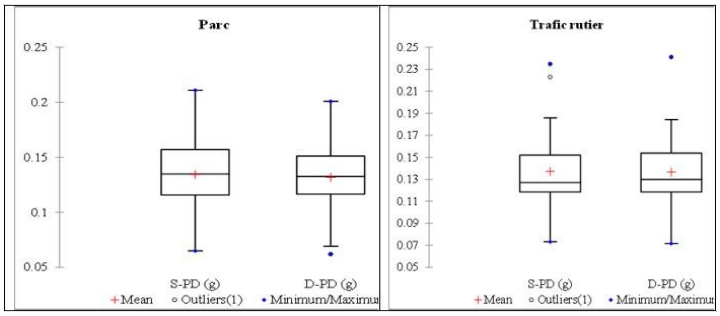

Figure 4.2. Boxplot diagram of the descriptive statistics of the weight (g) of pine needles in the clean area compared to areas with road traffic.

Washed and dehydrated samples

The results obtained from the measurements of the weights of the dehydrated and washed samples showed that, in the areas with traffic, both for L – SD and for R – SD, the average values were slightly lower (0,069 – 0,068) compared to the park area (0,077 – 0,076), but with a slightly higher standard deviation (Table 4.5.). Thus, the variability of needle weighing results in dehydrated conditions in traffic areas was higher. It should be noted, however, that both the minimum and maximum samples from traffic areas were lower than those collected from the park. Conversely, in a comparative analysis of the values of the left-sided needles with the values of the right-sided needles, in both types of zones, the left-sided samples were superior (Table 4.5.).

Table 4.5. Descriptive statistics of weight (g) of needles washed with distilled water and dehydrated.

	Park		**Road traffic**	
Statistic	**L-SD (g)**	**R-SD (g)**	**L-SD (g)**	**R-SD (g)**
Minimum	0,058	0,057	0,038	0,037
Maximum	0,109	0,105	0,106	0,103
Average	0,077	0,076	0,069	0,068
Standard deviation (n-1)	0,013	0,011	0,014	0,012

Regarding the weight of the dehydrated samples from the park areas compared to those from the road traffic areas, it is observed that the variant of the needles on the left side

had a larger range of values. Regarding the weight of the needles on the right, the boxplot diagram highlighted the presence of several outliers (outliers – marked by circles), suggesting that there were samples with significantly different sizes from the rest of the data.

In traffic areas, the whiskers have different lengths between the left and right sides, indicating some variability in the spread of the data. Thus, the needles on the right showed a lower variability compared to those on the left. In both types of zones, the samples on the right showed more extreme values.

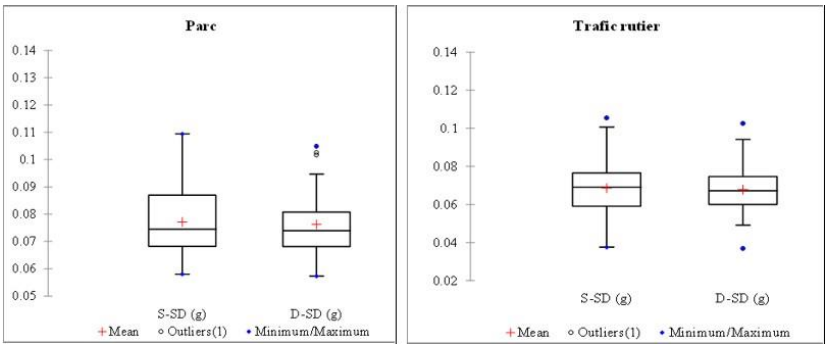

Figure 4.3. Boxplot diagram on the descriptive statistics of the weights (g) of the dehydrated and washed samples from the clean area compared to the areas with road traffic.

Fisher's variance test between 2 sets of data: left needle (park areas compared to road traffic areas), and right needle (park areas compared to road traffic areas).

Results indicated significant differences in left-sided needle sizes (p (< 0,0001) and right-sided needles (p (< 0,0001)). From the ratio between the variants of the two samples (Table 4.6.), it was observed that the difference between the variants of the two samples, the park area and the areas with road traffic, was greater for those on the left side (by 3,639 ×) compared to those on the right (of 0,275 ×). In contrast, from analyses of washed and dehydrated samples as well as fresh and sedimented (unwashed) samples, no influences of zones on needle weights were found.

Table 4.6. Results of Fisher tests to assess the differences between samples collected from the park and samples from road traffic areas (left-hand and right-hand pins).

	L-PD	R-PD	L-SD	R-SD	L-PSmm	R-PS mm
Ratio	1,480	1,449	0,830	0,790	3,639	0,275
F (Observed Value)	1,480	1,449	0,830	0,790	3,639	0,275

F (Critical Value)	1,762	1,762	1,762	1,762	1,762	1,762
DF1	49	49	49	49	49	49
DF2	49	49	49	49	49	49
p-value (Two-tailed)	0,174	0,198	0,518	0,413	**< 0,0001**	**< 0,0001**
Alpha	0,05	0,05	0,05	0,05	0,05	0,05

Fisher's variance test between 2 sets of data (left needle vs. right needle in park areas and left vs. right needle in road traffic areas).

Fisher's tests of variance between the weight and size of right-sided needles compared with left-sided needles revealed no significant differences. Even if the ratio between the variants of the two samples (left and right) per each sample variant (areas in the park, areas with traffic) showed slight differences between them, the results did not reach the minimum threshold of significance ($p < 0,05$).

Table 4.7. Results of Fisher's tests to assess differences between left needles versus right needles.

	Park			**Road Traffic**		
	PN	**DS**	**PS mm**	**PN**	**DS**	**PS mm**
Ratio	1,140	1,286	0,997	1,116	1,224	0,997
F (Observed Value)	1,140	1,286	0,997	1,116	1,224	0,997
F (Critical Value)	1,762	1,762	1,762	1,762	1,762	1,762
DF1	49	49	49	49	49	49
DF2	49	49	49	49	49	49
p-value	0,649	0,382	0,992	0,703	0,482	0,992
Alpha	0,05	0,05	0,05	0,05	0,05	0,05

Fresh samples

In general, needles from road traffic areas had larger sizes and weights, but with less variability compared to needles from the park area. These differences suggest that both pollution and other environmental factors in trafficked areas influence needle growth and development, leading to a different needle profile compared to those in cleaner areas.

Lower values observed in park samples reflect more favorable environmental conditions and healthier growth of pine needles, while higher values and the presence of outliers in areas with road traffic indicate the negative and variable influence of pollution

and other stress factors on the development of those and also the fact that individuals reacted disproportionately to pollution or other factors, specific to road traffic.

Washed and dehydrated samples

Weight of washed and dehydrated needles after weighing showed mean values to be lower in traffic areas but with slightly greater variability, which may indicate a more complex impact of pollution on these samples. Those on the left side generally had higher values than those on the right side, both in park areas and in those with traffic, and the presence of outliers was more pronounced in areas with road traffic, indicating a significant effect of these environmental conditions on the data distribution.

The study demonstrates **the influence of the polluted urban environment on the characteristics of pine needles, both in terms of their size and weight**, highlighting the need for careful monitoring of these indicators in assessing the impact of pollution on urban vegetation.

Even though the results of descriptive statistics revealed differences between the tested samples reflected by values of minimums, maximums, averages, and boxplot diagrams, Fisher analysis indicated that the variability between them was small, thus some of these measurements did not reach the minimum significance threshold ($p<0,05$) required.

However, the significant differences between the needle sizes in the park and road traffic areas as well as the Variance Ratio showed that **the variability of the left side needle sizes was much higher in the road traffic areas compared to the left side in parks**.

It is important to note that the higher variance observed for the needles in the road traffic area (especially for those on the left side) indicates a higher frequency of these needle variants in this area. This may reflect variations in environmental conditions (for example pollution) that affect the uniformity of needle growth.

In contrast, the analysis revealed that needle weight was not influenced by the trees' exposure to traffic pollution. The lack of significance for weight may be explained by the fact that although size varies, needle mass is not influenced in the same way, which may reflect an adaptation of the trees to stress conditions.

Lack of significant results regarding Left Needles vs Right Needles in the same area

The similarity between the left and right needles can be explained by the fact that although slight differences were observed between the two types of samples, they were not

sufficient to reach the threshold of statistical significance. Thus, it is likely that natural variability and environmental factors were not sufficiently different to produce more significant differences in size and weight between the two varieties of needles of the species selected for study.

4.2. LEAF MICROMORPHOLOGY MODIFICATIONS

The results of the scanning electron microscopy (SEM) studies showed that the samples collected from areas with intense road traffic in Bucharest present changes in leaf micromorphology compared to those collected from areas less exposed to atmospheric pollution. Deviations from normal micromorphology include:

- premature changes in the configuration of the wax layer;
- peri-stomatal thickenings similar to "Florin rings";
- epidermal cells with cutinized walls and irregular leaf surfaces;
- premature alteration of the structure of the stomatal complex;
- erosion of intra-stomatal wax deposits;
- abnormal serrations.

4.2.1. Premature changes in the configuration of the wax layer

In conifers, epicuticular wax is produced and deposited on leaf surfaces during leaf maturation. It is produced intensively in leaves younger than 1 year, with less intensity in 2-year-old leaves and almost none in mature ones that are 3 years old.

Young leaves collected from unpolluted areas have epicuticular wax deposited in the form of a dense network of microtubules concentrated especially in the area of the stomata (Fig.4.4.a,b).

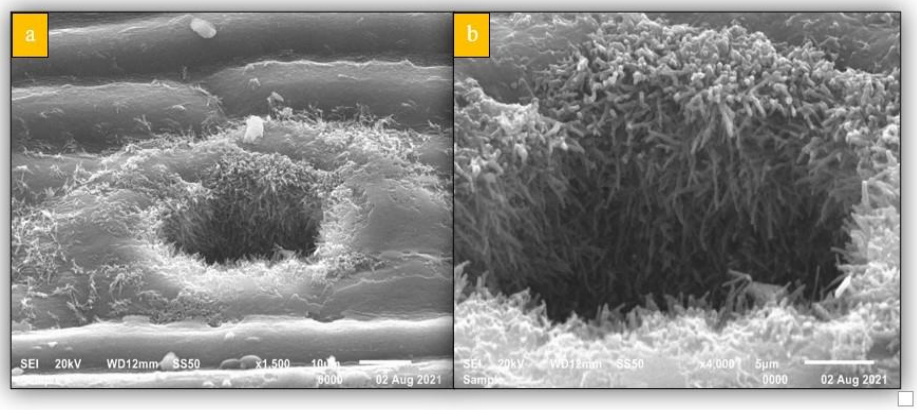

Figure 4.4. Normal distribution of epicuticular wax on 1-year-old leaves - material collected from Câmpina city *a* - general aspect; *b* - detail.

Under stress conditions caused by different atmospheric pollutants, the rate of wax production cannot compensate for its degradation, so alterations become visible even in 1-year-old leaves. These degradations were observed in all young leaf samples and consisted of the compaction of the tubule network by fusing together.

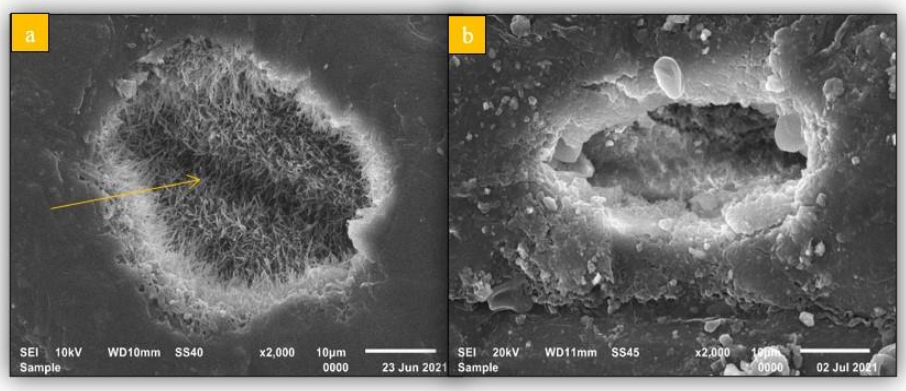

Figure 4.6. Early alterations of the network structure of the wax tubules, in 1-year-old leaves, *a* – visible median slit, early stage of alteration; *b* – deep alterations.

In fully matured leaves, the early degradations of the cuticular wax are much more visible and are characterized by a completely amorphous appearance, both at the periphery of the suprastomatal chamber aperture and inside it. Moreover, the wax deposited peripherally, during leaf ripening, destructures, and "falls" clogging the suprastomatal chamber (Fig.4.7.a,b).

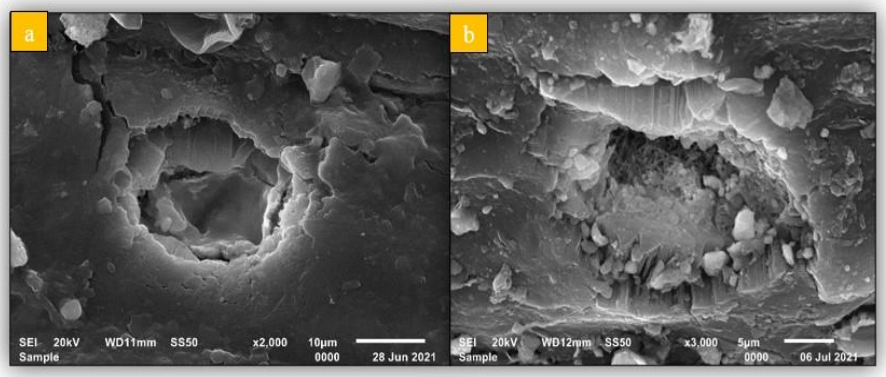

Figure 4.7. Advanced alterations of the cuticular wax in mature 2-year-old leaves *a* - destructured wax that almost completely clogs the suprastomatal chamber, *b* - fully clogged suprastomatal chamber.

4.2.2. "Florin rings"-like peri-stomatal thickenings

In samples where the particle deposition is consistent and the suprastomatal chamber is clogged, a circular thickening following the outline of the stomata was observed (Fig.4.9.).

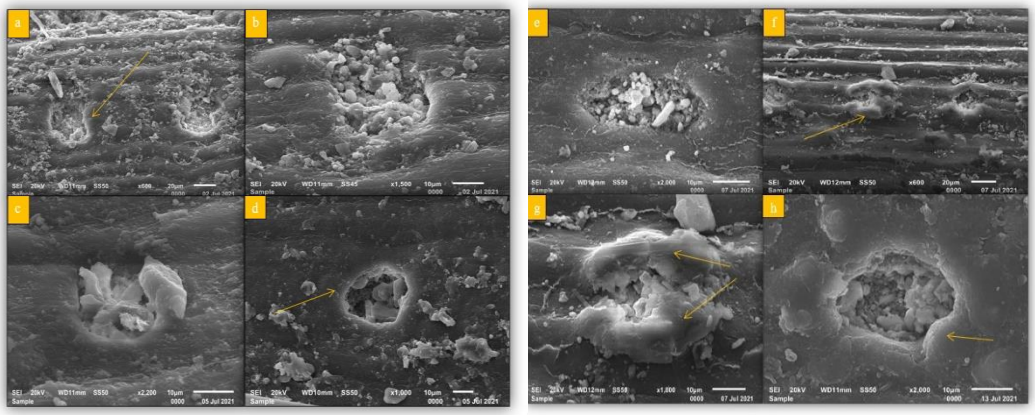

Figure 4.9. Peristomatic thickenings in samples from various origins *a, b* – material collected from the Ghimeș Entrance area (sector 5, Bucharest); *c, d* – material collected from the Șoseaua Olteniței area (sector 4, Bucharest) Stomata with deposits and peristomatic thickenings - *e, f, g*- material from the Bd. Unirii area (Sector 3, Bucharest) *h*- material from the Bd. N. Bălcescu area (Sector 1, Bucharest).

These thickenings are either discrete but visible (Fig. 4.9.a, b, c, d) or very elevated and obvious (Fig.4.9. e, f, g, h.).

The peri-stomatal thickenings prevent the wide opening of the ostioles, having a role in the regulation of water elimination through the stomata (Pautov *et al*., 2017) and the presence of these peristomatic "borders" can change the direction of growth of the hyphae, thus reducing the chances of their penetration through the ostiolar opening (Mohammadian *et al.,* 2009).

4.2.3. Epidermal cells with cutinized walls, irregular leaf surfaces

In all the samples where the leaf surfaces are populated by deposits, the external walls of the epidermal cells are convex showing thickenings and accentuated cutinizations that give a general striated relief, atypical for the leaves of the *P. Nigra* species.

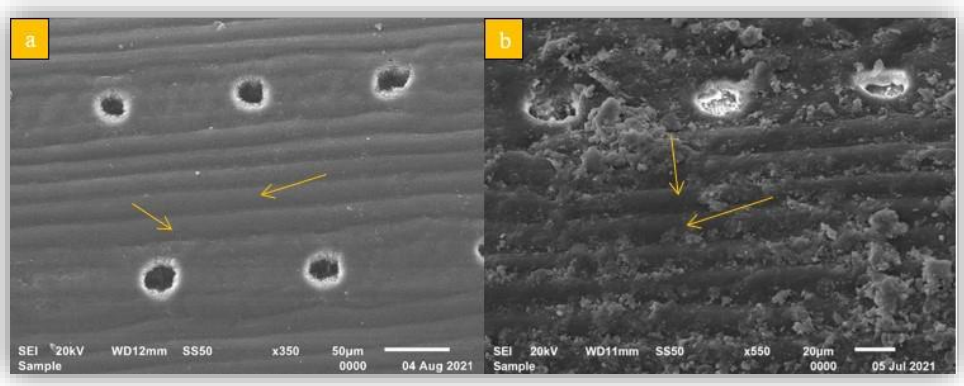

Figure 4.12. *a* – normal thickenings, almost uniform relief (control sample collected from the Câmpina area); *b* – exaggerated thickenings of the external walls of the epidermal cells, very uneven epicuticular relief.

4.2.4. Premature alteration of the structure of stomatal complex

In all the samples collected from areas with intense traffic, the compromise of the functioning of the stomatal complex could be observed by the complete clogging of the suprastomatal chamber with deposits.

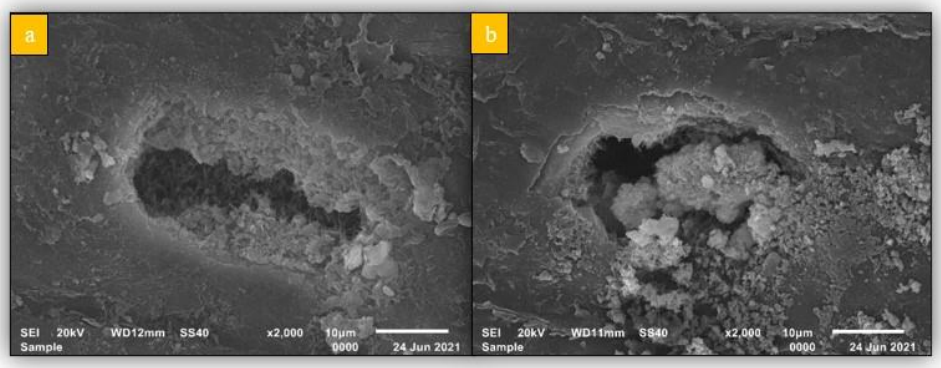

Figure 4.13. *a* – early clogging, microtubules are visible in the depth; *b* – combined wax-deposition clogging, parietal microtubule islands are visible.

As the leaf matures, the intrastomatal wax compacts until it forms true plugs that limit gas and water exchange (in leaves over 2 years old). The stomatal apparatus plays an important role in essential physiological processes such as photosynthesis, respiration and transpiration.

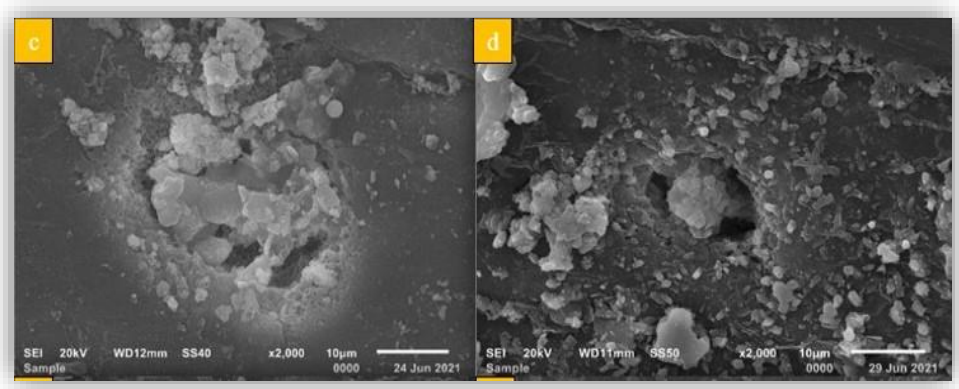

Figure 4.14. *c* and *d* – Clogging of the suprastomatal chamber in immature leaves.

4.2.5. Erosion of intra-stomatal wax deposits

The formation of wax plugs is a normal physiological process in conifers and occurs in fully matured needles. These structures mainly serve to limit water loss through transpiration (Brodribb and Hill, 1997) and to reduce the chances of endogenous fungal contamination by preventing their entry through the ostioles (Deckert *et al.*, 2001; Mohammadian *et al*., 2009).

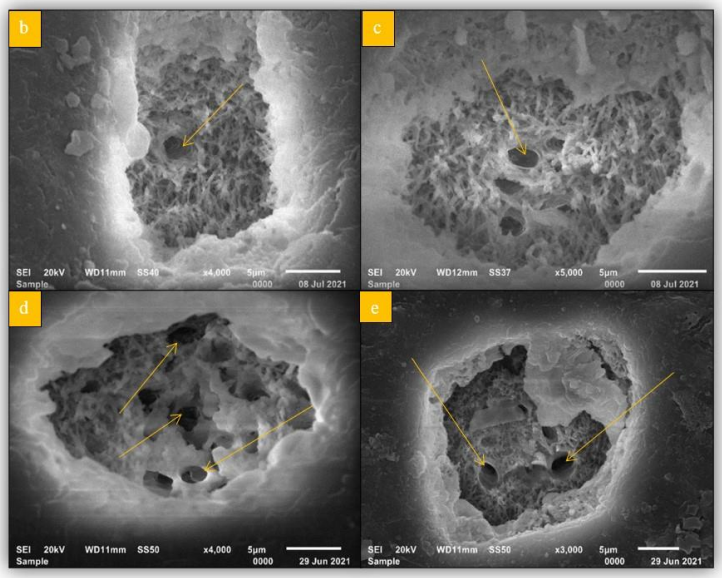

Figure 4.16. *b*, *c*, *d*, and *e* – perforations of the wax plugs in the early stage of formation.

4.2.6. Abnormal serrations

One of the most interesting micromorphologies visible in mature 2-3-year-old needles was the presence of epidermal denticles in the middle area of the limbus, structures that outline the onset of additional serrations in an area where serrations are normally absent.

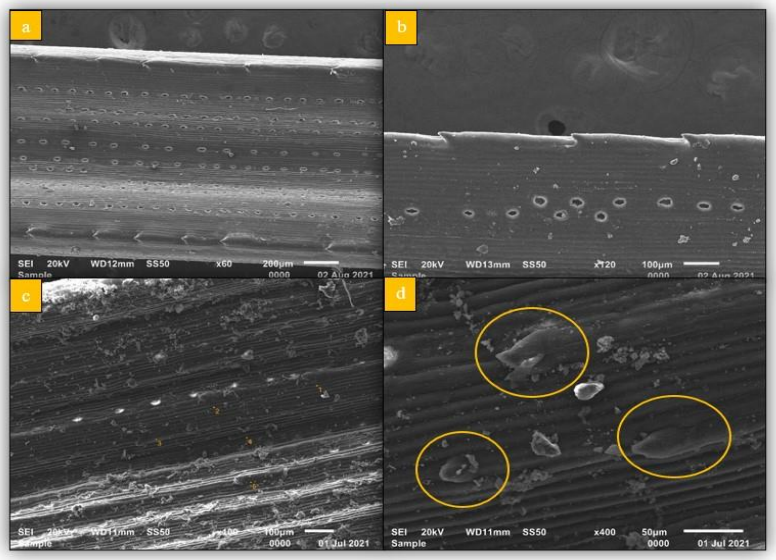

Figure 4.19. *a* – limb appearance with normal serrated edges (Control sample, Câmpina); *b* – detail of normal limb with serrated edge (P .control Câmpina); *c* - median, atypical serrations; d – detail of denticles.

4.2.7. Colonization with fungi

Colonization with fungi does not represent a deviation from the micromorphology of the species but may represent one of the consequences of changes in the structure of the epicuticular wax. In the specialized literature, numerous studies demonstrate that gaps in the compact structure of the cuticular wax favor fungal colonization and infections. Moreover, the presence of fungal infections is considered to signal that the cuticle wax is significantly affected (Grodzińska-Jurczak, 1998).

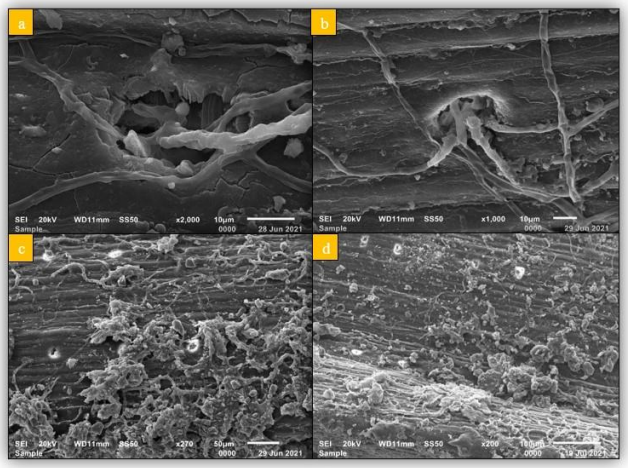

Figure 4.24. *a*, *b* – Penetration of hyphae inside the stomata; *c, d* – massive colonization with fungi.

4.3. FOLIAR STRUCTURES MODIFICATIONS

The observations made on the optical microscope of the cross-sections revealed a series of structural changes in the samples from polluted areas. These changes include the formation of an increased number of resinous canals, degeneration of liberian tissues, hypertrophy of Strasburger cells, and accumulation of phenolic compounds in various tissues. These changes were observed in almost all the samples analyzed and affect structures involved in defense mechanisms (resiniferous canals), in maintaining the water balance (stomata), in the transport of water and assimilates (conductive tissues – xylem and phloem), as well as associated structures such as endoderm, Strasburger cells, and sclerenchyma sheath.

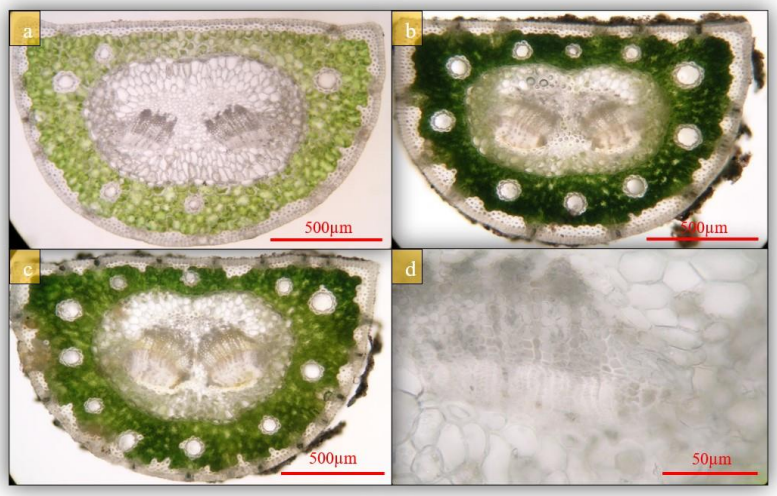

Figure 4.25. *a* – Resinous canals – normal aspect of the material collected from the Câmpina area; *b, c* – Increased number of resiniferous canals in samples collected from polluted areas; *d* – detail of conducting bundle with intact phloem and xylem (material collected from the Câmpina area).

Phenolic compounds usually accumulate in vacuoles in the form of hydrophilic conjugates. There are numerous studies on the correlation between the total phenolic content of conifer needles and exposure to various sources of pollution. Furthermore, the concentration of total phenolic compounds in conifer leaves is considered a biological indicator of air quality (Pasqualini *et al*., 2003). In the samples we analyzed, deposits of phenolic compounds were frequently observed in several tissue categories: conductive – in phloem cells, vessels and mechanical wood parenchyma cells – in the perifascicular sclerenchyma sheath and in the assimilating hypodermic collenchyma – in the cells of

parenchymal assimilating mesophyll – in the transfusion parenchyma and some protective tissues – endodermal cells.

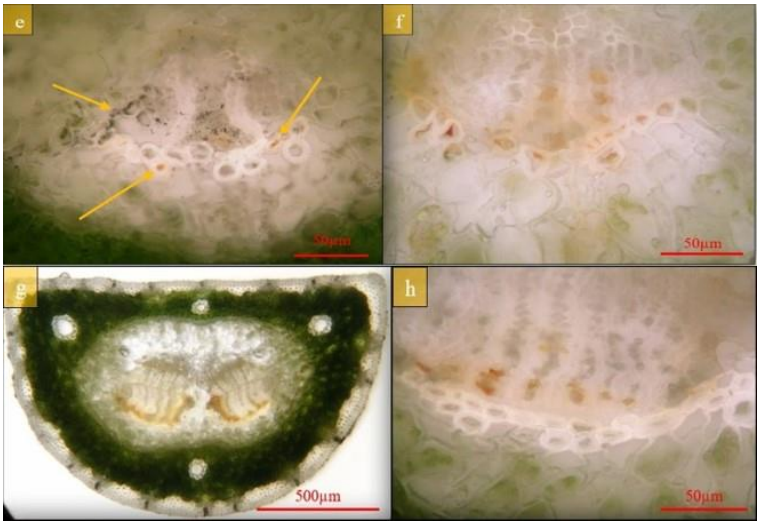

Figure 4.27. *e* – sclerenchyma cells with polyphenols, small cavities resulting from the disintegration of liberian vessels; *f* – phloem degeneration and accumulation of polyphenols in sclerenchyma cells; *g* – general appearance phloem degeneration; *h* – detail of phloem degeneration.

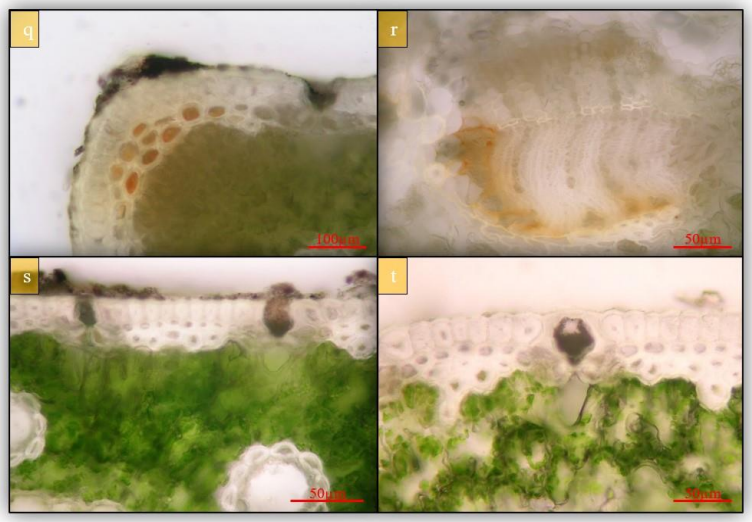

Figure 4.30. *q* – accumulation of polyphenols in the collenchyma cells (near the deposits); *r* – phloem degeneration detail; *s* – detail of deposits in the supra-stomatal chamber; *t* – stomata clogged with deposits, detail.

4.4. CHARACTERIZATION OF THE MAIN TYPES OF DEPOSITS

Two methods were used to identify the component elements of the deposits observed on the surface of the analyzed samples: *Elemental analysis by X-ray fluorescence spectrometry (XRF)* and *Elemental analysis by energy dispersive X-ray spectroscopy (EDX)*.

The elemental analysis by X-ray fluorescence spectrometry (XRF) allowed the evaluation of the total content of metals deposited on the leaf surfaces of the analyzed samples.

Table 4.8. The metal content of deposits on leaf surfaces.

Samples/ Metal content of deposits	P1	P2	P3	P4	P5	P6	P7	P8	P9	P10
Al	-	8.75	17.06	-	3.90	8.79	3.44	3.95	-	10.71
K	-	-	-	145.49	24.89	-	-	-	65.10	-
Ca	56.31	-	-	24.56	28.86	-	-	51.37	50.38	-
Ti	4.59	-	-	-	-	-	-	27.54	79.95	-
V	-	16.83	-	-	30.86	23.76	-	-	-	-
Mn	-	34.21	-	18.65	12.84	-	-	-	-	-
Fe	2.67	77.98	30.96	-	-	43.36	13.76	30.28	61.85	103.82
Co	-	-	-	-	-	-	-	4.96	-	-
Ni	-	-	7.04	-	-	-	-	-	-	-
As	-	-	9.17	7.70	-	-	3.99	-	-	3.70
Sr	-	1.66	-	-	-	-	5.53	-	8.01	-
Cr	-	-	14.79	-	-	-	8.28	-	-	10.61
Ge	-	-	-	-	11.40	-	6.86	-	-	-
Y	-	-	4.90	-	-	-	4.54	-	7.14	-
Ce	-	-	73.44	-	-	-	-	-	-	49.40
Cu	-	-	-	8.41	-	6.25	6.63	-	10.14	-
Zn	-	-	-	-	8.28	-	5.70	8.67	-	-

The samples that had the highest content of Strontium, Yttrium, Copper and Titanium were those collected from the Piața Victoriei area - Sector 1 (P9); the samples that accumulated the highest amounts of Aluminum, Chromium, Cesium, Arsenic and Nickel are those that came from the Ghimeș Entrance - Sector 5 (P3) area; the samples with the highest accumulations of Vanadium and Germanium were taken from the area of Olteniței Road - Sector 4 (P5); the samples in which the highest concentrations of Cobalt and Zinc were recorded were those that came from the area of Nicolae Bălcescu Bvd. - Sector 1 (P8), and those in which the highest amounts of Iron, Manganese, Potassium and , respectively Calcium were the samples taken from the Piața Iancului area - Sector 2 (P10), Iuliu Maniu Boulevard - Sector 6 (P2), Pieptănari Boulevard - Sector 5 (P4) and Virtuții Street - Sector 6 (P1), respectively.

Elemental analysis using energy-dispersive X-ray spectroscopy (EDX) allowed us to target discrimination of the elemental composition of the various types of deposits observed on the surface of the analyzed samples.

According to appearance, morphology, and elemental composition, the deposits could be grouped into several categories:

Crystalloid particles of 2-5 µm, with an irregular appearance

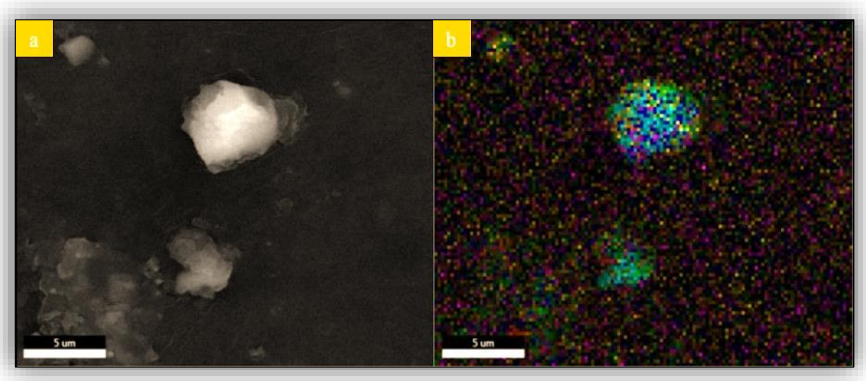

Figure 4.32. *a* – SEM micrograph; *b* – diagram of the layout of the component elements.

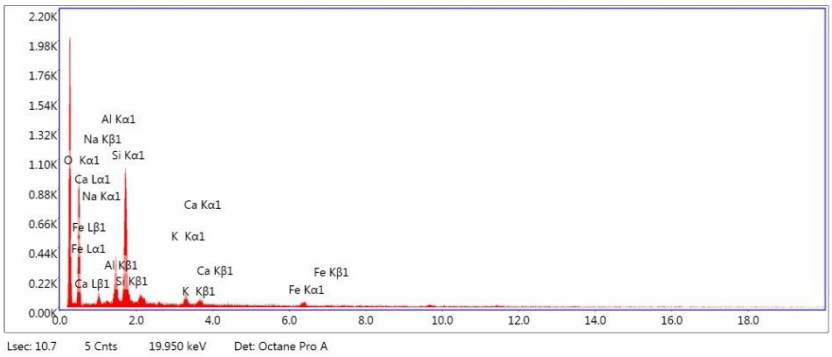

Figure 4.33. EDX spectrum of the component elements.

According to the data in Figure 4.33., these types of particles mainly contain Silicon, Aluminium and Sodium, and, to a lesser extent, Calcium, Potassium, and Iron.

Crystalloid particles in the form of compound prisms with a star-like appearance

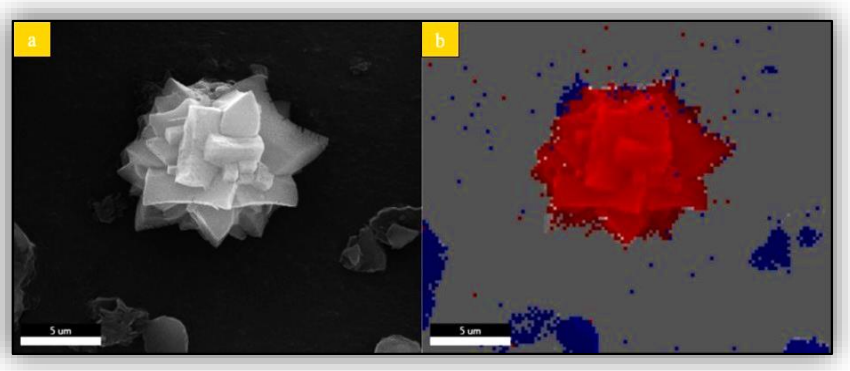

Figure 4.37. *a* –SEM micrograph, *b* – diagram of the layout of the component elements.

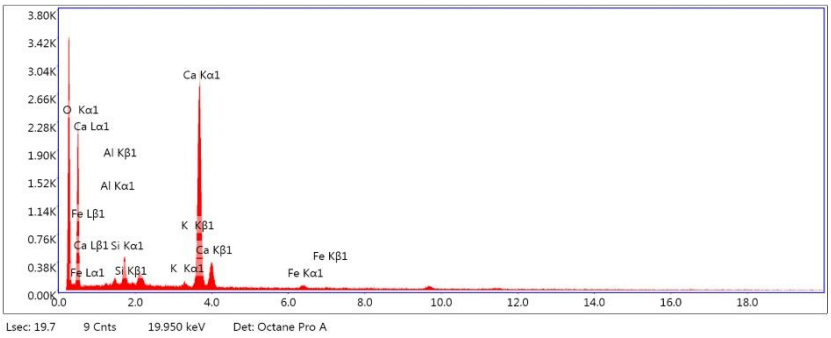

Figure 4.38. EDX spectrum of the component elements.

The data obtained showed that these types of particles are mainly composed of Calcium and, to a lesser extent, of Silicon and traces of Aluminum, Iron, and Potassium.

Crusty deposits of irregular prismatic shape

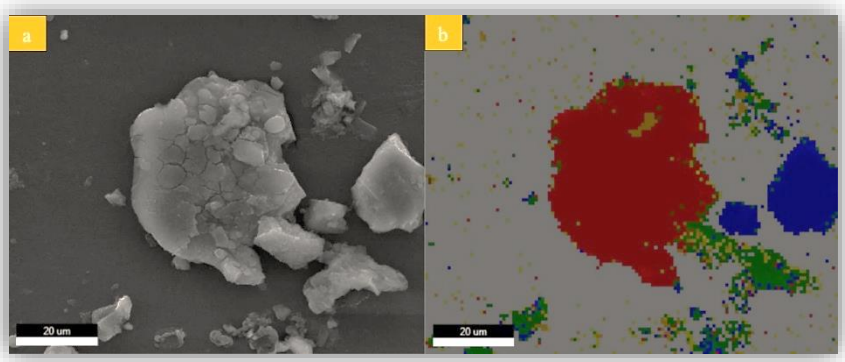

Figure 4.46. *a* – *a* –SEM micrograph, *b* – diagram of the layout of the component elements.

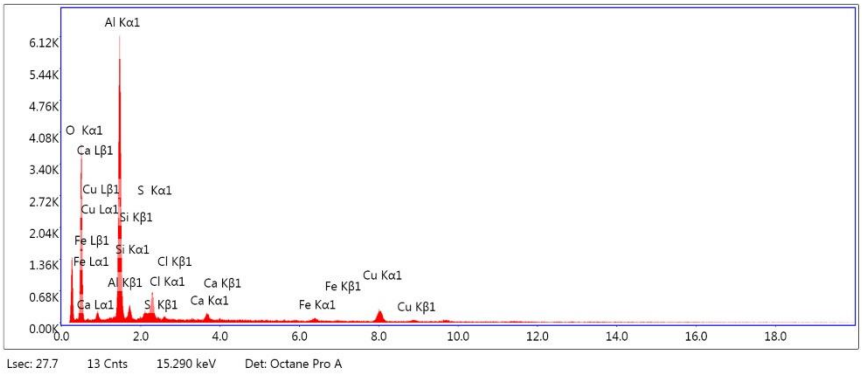

Figure 4.47. EDX spectrum of the component elements.

The EDX analysis data demonstrate that such particles consist mainly of Aluminium and, to a lesser extent, of Sulphur, Copper, and Silicon.

Compact amorphous aggregates

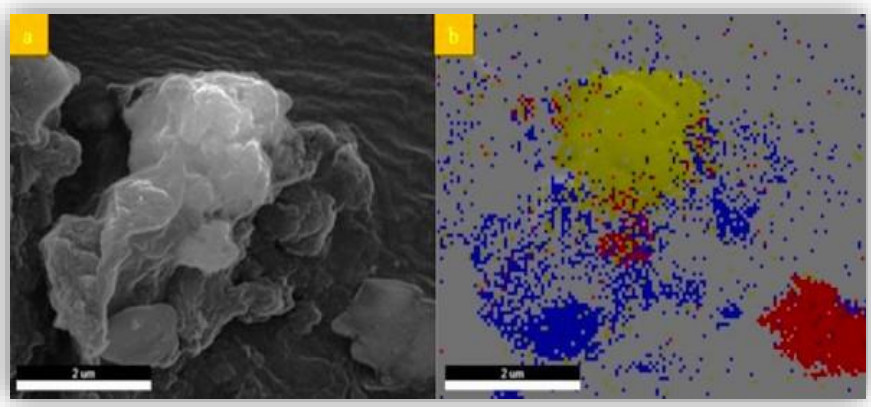

Fig 4.53. *a* – *a* –SEM micrograph, *b* – diagram of the layout of the component elements.

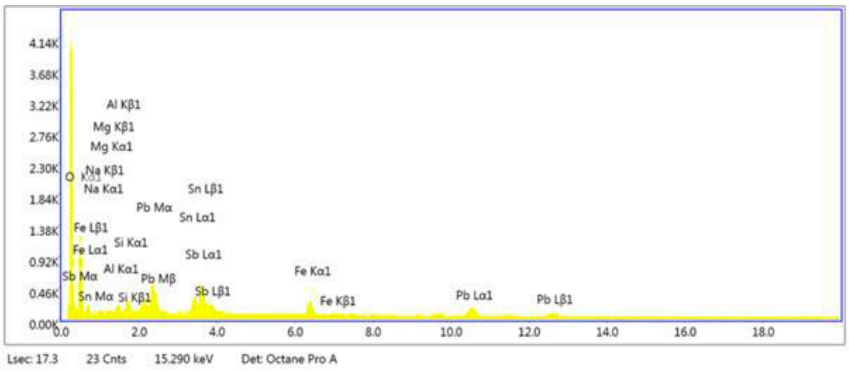

Figure 4.54. EDX spectrum of the component elements.

EDX analysis demonstrated that such deposits have a complex elemental composition in which Lead predominates, along with Stibiu and Tin, but also contain, to a lesser extent, Sodium, Aluminium, Silicon, Iron, and Magnesium.

Fine-grained compact aggregates

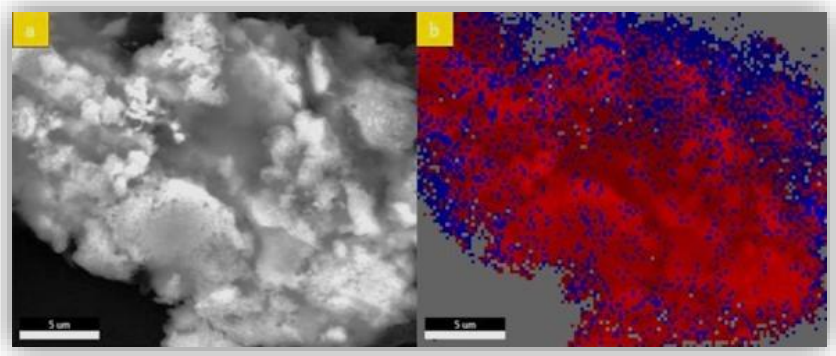

Figure 4.57. *a* – *a* –SEM micrograph, *b* – diagram of the layout of the component elements.

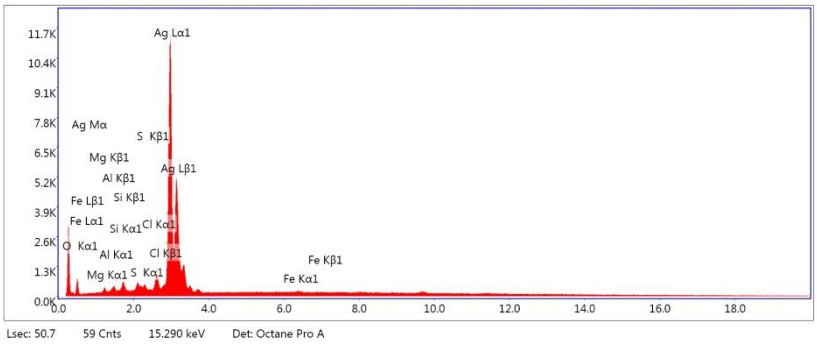

Figure 4.58. EDX spectrum of the component elements.

The data obtained from EDX analysis showed that such deposits are predominantly made of Silver and contain only traces of Silicon, Sulfur, Chlorine, Aluminum, Iron, and Magnesium.

Deposits in the form of compact prismatic crystals

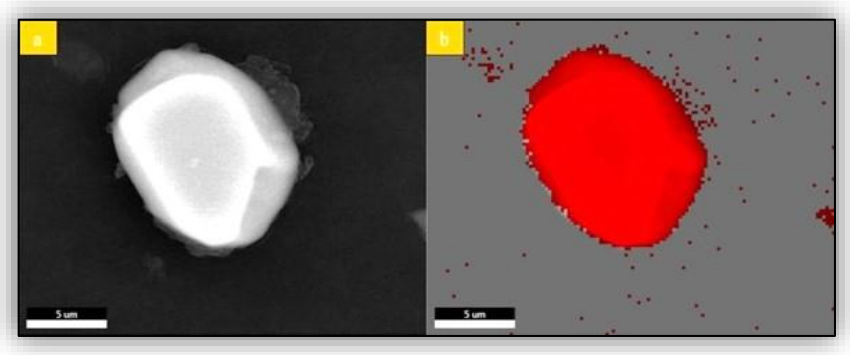

Figure 4.59. *a* – *a* –SEM micrograph, *b* – diagram of the layout of the component elements.

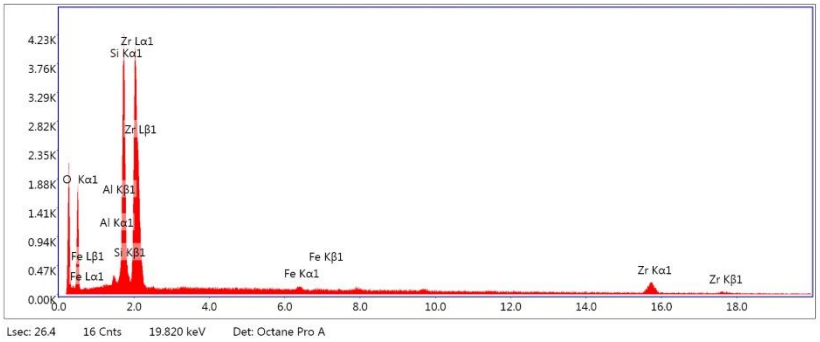

Figure 4.60. EDX spectrum of the component elements.

The results of the EDX analysis demonstrated that these types of particles are mainly composed of Zirconium, but also of smaller amounts of Silicon, as well as traces of Aluminium and Iron.

Particles in the form of microspheres

A category of particles frequently observed in deposits on the surface of black pine needles was represented by small spherical formations (0,5-3 μm). This type of microparticles, although they present a very similar micromorphology characterized by a smooth-glassy appearance, have a slightly different elemental composition that allowed us to classify them into 5 types as follows:

- Microspheres containing mainly Aluminium and Magnesium (Figure 4.63 A). EDX analysis indicated that the microspheres have a high content of Aluminium and Magnesium, but also Silicon, Sodium, and Barium, in smaller amounts.

- Microspheres with Silicon and Aluminium (Figure 4.63. B). EDX analysis indicated that such microspheres have a high content of Silicon, Aluminium and Sodium, in smaller amounts, as well as traces of Iron, Magnesium, Potassium, and Calcium.
- Microspheres with a high content of Silicon and Sodium (Figure 4.63. C). EDX analysis indicated that such microspheres have a high content of Silicon and Sodium, but also Aluminium, Iron, Calcium, and Magnesium, but in smaller quantities.
- Microspheres mainly made of Silicon and Aluminium (Figure 4.63. D).

EDX analysis indicated that such microspheres have a high content of Silicon and Aluminium, but also low amounts of Sodium, Iron, and Magnesium.

- Microspheres formed mainly of Silicon (Figure 4.63. E).

EDX analysis indicated that such microspheres have a high content of Silicon and Aluminium in a smaller amount, but also Sodium, Iron, and Potassium.

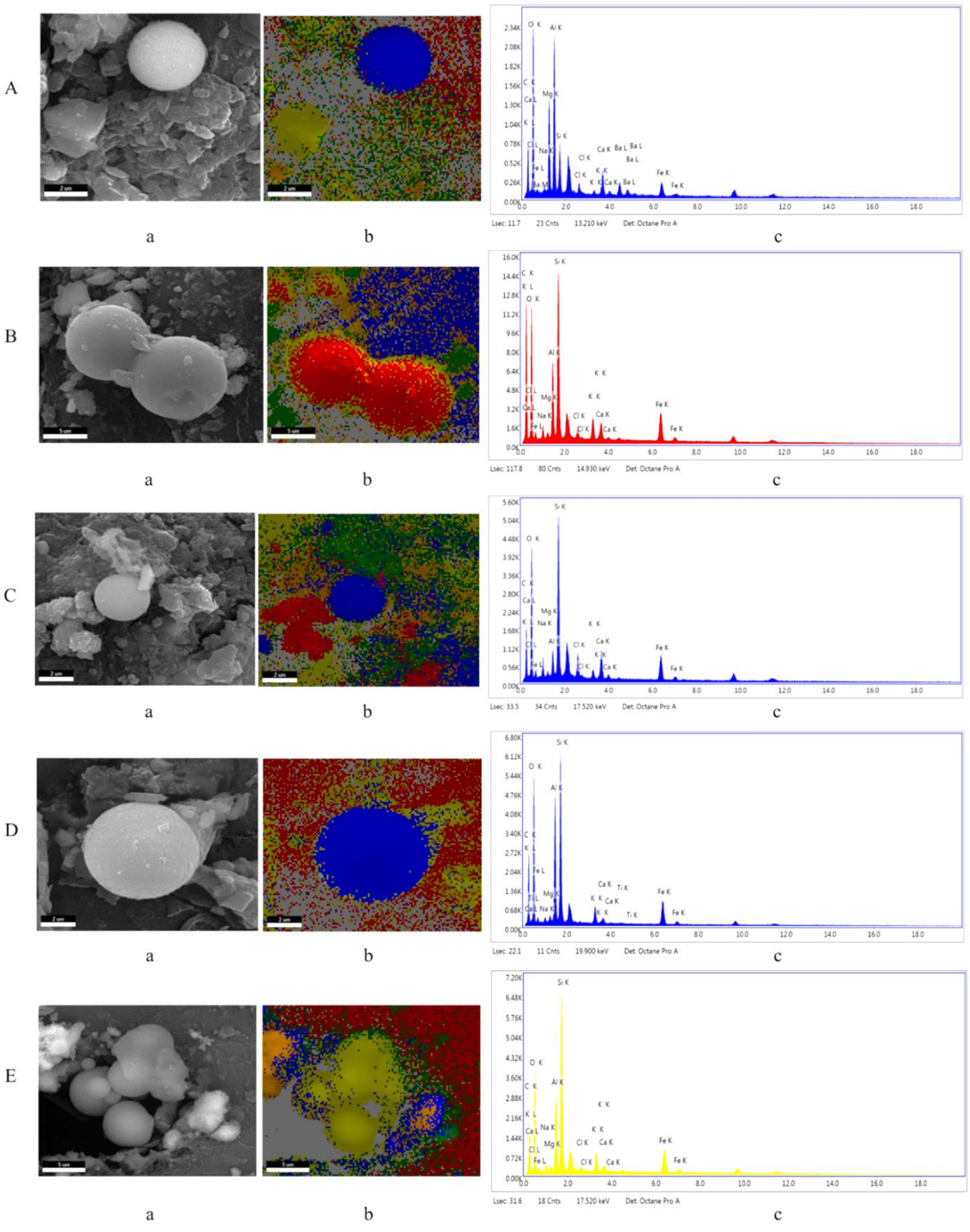

Figure 4.63. **A** – Microsphere Al-Mg, **B** – Microsphere Si-Al-Na, **C** – Microsphere Si-Na, **D** – Microsphere Si-Al, **E** – Microsphere Si-Al-Na-Fe (*a* – SEM micrograph, *b* – EDX diagram, *c* – EDX spectrum).

Other types of particles

During scanning electron microscope investigations, sveral types of particles were observed that could not fit into any of the previously described categories. Most likely, these micro-fragments fall into the category of microplastics.

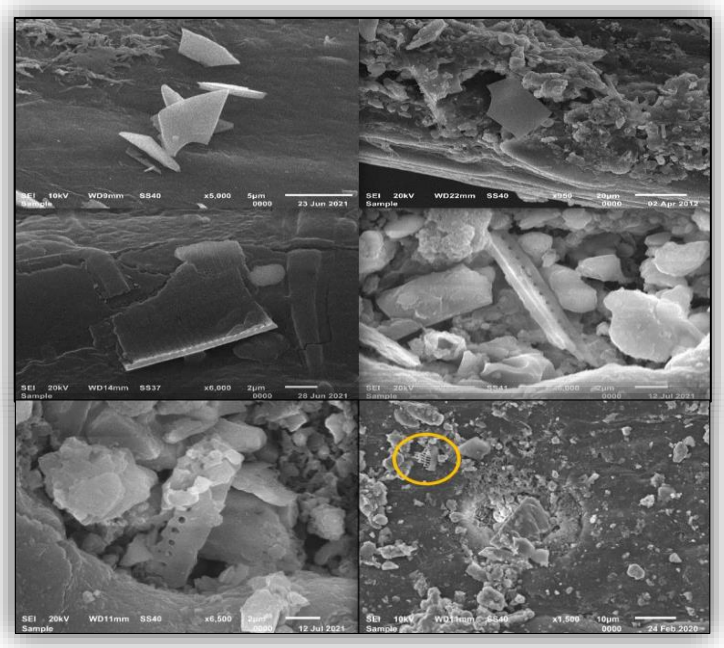

Figure 4.64. Microfragments of anthropogenic origin.

The EDX analysis of such types of microparticles revealed that they are formed mainly of Silicon, but also of small amounts of Aluminum and Sodium, as well as traces of Iron and Magnesium.

In the results presentation of the EDX analysis, only the graphs and diagrams associated with the particles of interest were selected. The extended results obtained from the EDX analyzes are presented in **Appendix 2**.

4.5. SYNTHESIS OF THE RESULTS

The morphological, micromorphological, and structural analysis of the samples revealed a series of deviations from the characteristics of the *Pinus nigra* species. These deviations consisted of a manifestation of the fluctuating asymmetry of the needles, premature changes in the configuration of the wax layer, peri-stomatal thickenings similar to "Florin rings", epidermal cells with cutinized walls, irregular leaf surfaces, premature alteration of the structure of the stomatal complex, erosion of intra-stomatal wax deposits,

abnormal serrations, additional resin canals, early phloem degradation, hypertrophy of Strasburger cells and accumulation of phenolic compounds.

Since these changes are stable, we consider that **they can constitute morphological and structural markers of pollution**. All the deviations from the normal structure identified by us are additional arguments that support and complement the existing data in the literature according to which **the black pine can be a useful indicator in the evaluation of the state of pollution in some areas**. The *Pinus nigra* species has been the subject of numerous complex studies through which it has been proven that it represents an efficient accumulator of metals, pesticides and polycyclic aromatic hydrocarbons (Kaya *et al*., 2010, Pavlovic *et al*., 2017, Baroudi *et al*., 2021, Zeiner *et al*., 2021, Chudzińska *et al*., 2014, Oleksyn *et al*., 1987, Rimondi *et al*., 2020, Piccardo *et al*., 2005, Klingberg *et al*., 2022, Parzych and Sobisz, 2012) that recommend both as a biomonitor species of air pollution (Baroudi *et al*., 2022, Katsidi *et al*., 2023, Chiarantini *et al*., 2016, Klánová *et al*., 2009, Rai, 2013, Zsigmond *et al*., 2021, Keskin and Ili, 2012, Berlizov *et al*., 2007), and as a green filter for reducing the degree of pollution (Koksal *et al.*, 2024, Petrova, 2020, Petrova, 2024, Juranovic *et al*., 2019). Black pine has been shown to react to atmospheric pollution through a multitude of response types including genetic and epigenetic levels (Katsidi *et al*., 2023).

Scanning electron microscope studies allowed the identification of deposits with various morphologies, ranging from prismatic crystalloids, loose or compact granular structures, crusts, films, amorphous aggregates, or microspheres.

The elemental analysis demonstrated that the particles identified on the samples analyzed by us have a diverse and complex composition that includes: Aluminum, Silicon, Calcium, Magnesium, Manganese, Iron, Phosphorus, Sulfur, Potassium, Lead, Yttrium, Zirconium, Stbium, Tin, Strontium, Silver, Cobalt, Titanium, Germanium, Cesium, Arsenic, Chlorine, Vanadium. Elements such as Zinc, Manganese, Vanadium, Barium, Aluminum, Zirconium, Yttrium, Cesium, Rubidium, Stidium, Tin, Barium, Chromium, Iron, and Copper are recognized as the main components of particles generated by road traffic (Hjortenkrans *et al.,* Guéguen *et al.,* 2012). The main sources of contamination in high-traffic areas are exhaust gases (especially Nickel and Zinc), particles generated by brake wear and tire wear. The main metals emitted from brake wear are thought to be Copper, Stumb, and Zinc, while Lead and Cadmium are considered historical residues emitted from the use of fuel additives (Johansson *et al*., 2009, Hjortenkrans *et al*., 2006). In addition, compared to the elements

reported in the literature as generated by road traffic, the analysis carried out by us also identified other elements such as: Zirconium, Stium, Tin, Strontium, Silver, Cobalt, Titanium, Germanium, Cesium, Arsenic, Chlorine, and Vanadium. These elements could also come from the wear of the braking systems because the materials used in their production are very diverse. Other activities, such as heat generation in thermal power plants or fireworks, can also generate a variety of airborne elements. For example, pyrotechnic displays generate particles containing Potassium, Barium, Strontium, Cadmium, Sulfur, and Phosphorus (Kumar *et al*., 2016).

A special category of deposits identified is represented by *microspheres*. Due to their small size, often below 3 μm, they fall under the category of 2.5 μm suspended particles, the so-called PM2.5. Currently, studies are published on the appearance and composition of particles resulting from exhaust gases (Chernyshev *et al*., 2018, Pallares *et al*., 2019, Wang *et al*., 2019, Chernyshev *et al*., 2018, Neer & Koylu, 2006), but perfectly spherical particles of such origin are not described in any study. Our results demonstrate that airborne microspheres can also originate from exhaust gases. Microspherical particles with the same appearance, size, and composition as those identified on the leaf surfaces were isolated in the material taken from inside the exhaust pipes of some vehicles with internal combustion engines using diesel and gasoline respectively (EDX reports are available in Appendix 2) . Due to their small size, these particles are at risk for a several conditions associated with PM2.5 including **respiratory, cardiovascular, neurological or dermatological diseases** (Valavanidis *et al*., 2008, Wu *et al*., 2019, Manisalidis *et al*., 2020, Zhang *et al*., 2015, Yang *et al*., 2020, Sierra-Vargas *et al*., 2023, Kim *et al*., 2020). Our results indicated that the microspheres resulting from the exhaust contain appreciable amounts of Aluminum (between 2,79% and 11,88% of the weight of the microsphere) which, inhaled together with the microsphere, can reach the circulatory system and from there into several tissues, including the cerebral. It is known that Aluminum can cross the blood-brain tissue barrier (hemato-encephalic), accumulating in brain areas that are rich in transferrin receptors (Inan-Eroglu & Ayaz, 2018). Currently, studies are available in which evidence is provided for the neurotoxic effect of Aluminum, which includes the formation of beta-amyloid plaque and neurofibrillary tangles – primary etiological factors in the setting of Alzheimer's disease (Exley, 2017, Exley & Clarkson, 2020).

5. CONCLUSIONS

1. *Pinus nigra* presents a series of qualities that recommend it as a biomonitor of air quality. These are: the increased resistance to atmospheric pollutants, the ability to adapt to the conditions of the urban environment, the manifestation of easily detectable responses under the action of atmospheric pollutants, and the frequency as a decorative species in the urban landscape, along road arteries in parks and in various types of green spaces
2. The manifestation of leaf asymmetry in black pine can be an indicator of exposure to pollution. This parameter is highlighted in the black pine by fluctuations in the weight and length of those pairs.
3. Obvious structural changes such as the development of additional resinous canals, degradation of phloem, hypertrophy of Strasburger cells, and accumulation of phenolic compounds in tissues that normally do not produce this type of compounds, can be indicators of exposure to pollution.
4. Premature alteration of the configuration of the wax layer, epidermal cells with uneven cutinized walls, irregular leaf surfaces, and premature alteration of the structure of the stomatal complex are manifestations of response to pollution and can be used as indicators of atmospheric pollution.
5. The abnormal median serrations identified on the leaf limb surface of *Pinus nigra* are structural aberrations reported for the first time in a conifer species and can be used as pollution biomarkers.
6. The presence of "Florin ring" type micromorphology is mentioned for the first time in the *Pinus nigra* species, and it can be an indicator of pollution.
7. Massive fungal colonization of leaf surfaces can be an indicator of erosion at the epicuticular level caused by various polluting agents.
8. All the identified indicators are biomarkers of pollution and can form the basis of quick and low-cost environmental quality assessment protocols.
9. *Pinus nigra* is an excellent study material for the identification of various airborne particles. Thick deposits of epicuticular wax immobilize a variety of airborne particles, with black pine trees acting as an effective "green filter".
10. The deposits on the leaf surfaces have a different appearance, structure and elemental composition, most containing Silicon and Aluminum but also Calcium, Magnesium, Manganese, Iron, Phosphorus, Sulphur, Potassium, Lead, Yttrium, Zirconium,

Antimony, Tin, Strontium, Gold, Silver, Cobalt, Titanium, Germanium, Cesium, Arsenic, Chlorine, Vanadium.

11. The main sources of contamination in high-traffic areas are exhaust gases, particles generated by brake wear, and tire wear. Added to these are other types of particles generated by anthropogenic activities such as coal burning or pyrotechnic shows.
12. The microspheres identified on the foliar surfaces of the needles exposed to intense traffic also come from the exhaust material of automobiles, both gasoline, and diesel, not only from the burning of coal as specified in the specialized literature.
13. The identified microspheres, due to their small size, are respirable and represent a high health risk, airborne microparticles being associated with the development of respiratory, cardiovascular, and neurological diseases.
14. Microspheres containing Aluminum once inhaled may present a risk for the development of structural abnormalities in the brain tissue that are recognized as precursors to the onset of Alzheimer's disease.
15. Simply assessing existing deposits on black pine needles can provide valuable information on airborne particles of increased health risk.

Bibliography

1. Baroudi, F., Al-Alam, J., Chimjarn, S., Haddad, K., Fajloun, Z., Delhomme, O. and Millet, M., 2022. Use of Helix aspersa and Pinus nigra as Bioindicators to study temporal air pollution in Northern Lebanon. *International Journal of Environmental Research*, *16*(1), p.4.

2. Baroudi, F., Al-Alam, J., Delhomme, O., Chimjarn, S., Fajloun, Z. and Millet, M., 2021. The use of Pinus nigra as a biomonitor of pesticides and polycyclic aromatic hydrocarbons in Lebanon. Environmental Science and Pollution Research, 28, pp.10283-10291.

1. Bartosz, G., 1997. Oxidative stress in plants. Acta Physiologiae Plantarum 19, 47e64.

3. Berlizov, A. N., Blum, O. B., Filby, R. H., Malyuk, I. A., & Tryshyn, V. V., 2007. Testing applicability of black poplar (Populus nigra L.) bark to heavy metal air pollution monitoring in urban and industrial regions. *Science of the Total Environment*, *372*(2-3), 693-706.
2. Brodribb, T., Hill, R.S., 1997. Imbricacy and stomatal wax plugs reduce maximum leaf conductance in southern hemisphere conifers. *Australian Journal of Botany* 45: 657–668. doi: 10.1071/bt96060.

3. Cape, J.N., 1994. Evaluation of pollutant critical levels from leaf surface characteristics in air pollutants and the leaf cuticle (pp. 123-138). *Berlin, Heidelberg: Springer Berlin Heidelberg.*

4. Chernyshev, V. V., Zakharenko, A. M., Ugay, S. M., Hien, T. T., Hai, L. H., Kholodov, A. S., Burykina, T.I., Stratidakis A.K., Mezhuev, Ya. O.,Tsatsakis, A.M., Golokhvast, K. S., 2018. Morphologic and chemical composition of particulate matter in motorcycle engine exhaust. Toxicology Reports, 5, 224-230
5. Chernyshev, V. V., Zakharenko, A. M., Ugay, S. M., Hien, T. T., Hai, L. H., Kholodov, A. S., Burykina, T.I., Stratidakis A.K., Mezhuev, Ya. O.,Tsatsakis, A.M., Golokhvast, K. S., 2018. Morphologic and chemical composition of particulate matter in motorcycle engine exhaust. Toxicology Reports, 5, 224-230.
4. Chiarantini, L., Rimondi, V., Benvenuti, M., Beutel, M.W., Costagliola, P., Gonnelli, C., Lattanzi, P. and Paolieri, M., 2016. Black pine (Pinus nigra) barks as biomonitors of airborne mercury pollution. *Science of the Total Environment*, *569*: 105-113.
5. Chudzińska, E., Diatta, J. B., & Wojnicka-Półtorak, A., 2014. Adaptation strategies and referencing trial of Scots and black pine populations subjected to heavy metal pollution. *Environmental science and pollution research*, *21*, 2165-2177.
6. Deckert, R.J., Melville, L.H., Peterson, R.L., 2001. Epistomatal chambers in the needles of *Pinus strobus* L. (eastern white pine) function as microhabitat for specialized fungi. *International Journal of Plant Sciences* 162: 181–189. doi: 10.1086/317905.

7. DuToit, S.H., Steyn, A.G.W. and Stumpf, R.H., 2012. Graphical exploratory data analysis. *Springer Science & Business Media.*

8. EEA, 2019. Air quality in Europe — 2019 report No 10/2019. *European Environment Agency (https://www.eea.europa.eu/publications/air-quality-in-europe-2019* - accessed on 20.07.2020).

9. EEA, 2019. Cutting air pollution in Europe would prevent early deaths, improve productivity and curb climate change *(http://www.eea.europa.eu/highlights/cutting-air-pollution-in-europe* - accessed on 8.06.2020).

10. Exley, C., 2017. Aluminium should now be considered a primary etiological factor in Alzheimer's disease. *Journal of Alzheimer's Disease Reports*, 1(1), 23-25.
11. Exley, C., Clarkson, E., 2020. Aluminum in human brain tissue from donors without neurodegenerative disease: A comparison with Alzheimer's disease, multiple sclerosis and autism. *Scientific Reports*, 10(1), 1-7.
12. Gill, M., 2014. Heavy Metal Stress in Plants: a review. *International Journal of Advanced Research, 2*(6), 1043-1055.

13. Gostin, I., 2007. Biomarkeri structurali la plante. *Editura Universităţii „Alexandru Ioan Cuza", Iaşi*. ISBN 9737032918, 184p.

14. Grodzińska-Jurczak, M., 1998. Conifer epicuticular wax as a biomarker of air pollution: an overview. *Acta societatis botanicorum Poloniae*, 67(3-4), p.291.

15. Guéguen, F., Stille, P., Dietze, V., Gieré, R., 2012. Chemical and isotopic properties and origin of coarse airborne particles collected by passive samplers in industrial, urban, and rural environments. *Atmospheric Environment*, *62*, 631-645.

16. Günthardt-Goerg, M.S. Vollenweider, P., 2007. Linking stress with macroscopic and microscopic leaf response in trees: new diagnostic perspectives. *Environmental pollution*, *147*(3), pp.467-488.
17. Heath, M.C., 2000. Hypersensitive response-related death. *Plant Molecular Biology* 44, 321e334.

18. Hjortenkrans, D., Bergbäck, B., Häggerud, A., 2006. New metal emission patterns in road traffic environments. Environmental Monitoring and Assessment, 117, 85-98.
19. Hjortenkrans, D., Bergbäck, B., Häggerud, A., 2006. New metal emission patterns in road traffic environments. *Environmental Monitoring and Assessment*, *117*, 85-98.

20. Honour, S.L., Bell, J.N.B., Ashenden, T.W., Cape, J.N., Power, S.A., 2009. Responses of herbaceous plants to urban air pollution: effects on growth, phenology and leaf surface characteristics. *Environmental pollution*, 157(4), 1279-1286.

21. Inan-Eroglu, E. and Ayaz, A., 2018. Is aluminum exposure a risk factor for neurological disorders?. *Journal of Research in Medical Sciences*, 23(1), p.51.
22. Iordanidis, A., Buckman, J., Triantafyllou, A. G., Asvesta, A., 2008. Fly ash–airborne particles from Ptolemais–Kozani area, northern Greece, as determined by ESEM-EDX. *International Journal of Coal Geology*, 73(1), 63-73.
23. Johansson, C., Norman, M., Burman, L., 2009. Road traffic emission factors for heavy metals. *Atmospheric Environment*, 43(31), 4681-4688.
24. Juranović Cindrić, I., Zeiner, M., Starčević, A. and Stingeder, G., 2019. Metals in pine needles: characterisation of bio-indicators depending on species. *International journal of environmental science and technology*, *16*(8), pp.4339-4346.

6. Katsidi, E.C., Avramidou, E.V., Ganopoulos, I., Barbas, E., Doulis, A., Triantafyllou, A. and Aravanopoulos, F.A., 2023. Genetics and epigenetics of Pinus nigra populations with differential exposure to air pollution. *Frontiers in Plant Science*, *14*, p.1139331.

25. Katsidi, E.C., Avramidou, E.V., Ganopoulos, I., Barbas, E., Doulis, A., Triantafyllou, A. and Aravanopoulos, F.A., 2023. Genetics and epigenetics of Pinus nigra populations with differential exposure to air pollution. *Frontiers in Plant Science*, *14*, p.1139331.

7. Kaya, G., Ozcan, C. and Yaman, M., 2010. Flame atomic absorption spectrometric determination of Pb, Cd, and Cu in Pinus nigra L. and Eriobotrya japonica leaves used as biomonitors in environmental pollution. *Bulletin of environmental contamination and toxicology*, 84, pp.191-196.

8. Keskin, N., and Ili, P., 2012. Investigation of particular matters on the leaves of Pinus nigra Arn. subsp. pallasiana (Lamb.) Holmboe in Denizli (Turkey). *Pak. J. Bot*, *44*(4), 1369-1374.
26. Kim, H., Kim, W-H., Kim, Y-Y., Park, H-Y., 2020. Air Pollution and Central Nervous System Disease: A Review of the Impact of Fine Particulate Matter on Neurological Disorders. *Frontiers in Public Health*, 8:575330.
9. Klánová, J., Čupr, P., Baráková, D., Šeda, Z., Anděl, P., & Holoubek, I., 2009. Can pine needles indicate trends in the air pollution levels at remote sites?. *Environmental Pollution*, *157*(12), 3248-3254.
10. Koksal, S. E., Kelleci, O., Tekingunduz, G., & Aydemir, D., 2024. The influence of road traffic and industrial plant-induced air pollution on the physical, mechanical, chemical and morphological properties of the black pine wood. *Maderas: Ciencia y tecnología*, 26(1), 1.

27. Kumar, M., Singh, R. K., Murari, V., Singh, A. K., Singh, R. S., Banerjee, T. 2016. Fireworks induced particle pollution: a spatio-temporal analysis. *Atmospheric Research*, 180, 78-91.
28. Mamedova, A.O. and Farzalieva, N.M., 2020. Pinus eldarica Medw. As indicator of vehicular pollution. *Вестник Нижневартовского государственного университета*, (1), pp.134-139.

29. Mammadova, A.O., 2009. Phytoindicatory and environmental quality management. *Annals of Agrarian Science*, 7(4), pp.58-60.

30. Manisalidis, I., Stavropoulou, E., Stavropoulos, A., Bezirtzoglou, E., 2020. Environmental and Health Impacts of Air Pollution: A Review. Frontiers in Public Health, 8:14.

31. Manninen, S. and Huttunen, S., 1995. Scots pine needles as bioindicators of sulphur deposition. *Canadian Journal of Forest Research*, *25*(10), pp.1559-1569.

32. Martín, J.R., De Arana, C., Ramos-Miras, J.J., Gil, C., Boluda, R., 2015. Impact of 70 years urban growth associated with heavy metal pollution. *Environmental pollution*, 196, 156-163.

33. Matyssek, R., Günthardt-Goerg, M.S., Maurer, S., Keller, T., 1995. Nighttime exposure to ozone reduces whole-plant production in Betula pendula. *Tree physiology*, *15*(3), pp.159-165.

34. Mohammadian, M. A., Hill, R. S. & Watling, J. R., 2009. Stomatal plugs and their impact on fungal invasion in Agathis robusta. *Australian Journal of Botany*, *57*(5), 389-395.

35. Nathanson, J.A., 2020. Air pollution. *Encyclopedia Britannica*, https://www.britannica.com/science/air-pollution. Accesat la 08-12-2020.

36. Neer, A., Koylu, U. O., 2006. Effect of operating conditions on the size, morphology, and concentration of submicrometer particulates emitted from a diesel engine. *Combustion and Flame*, 146(1-2), 142-154.

37. Pallarés, S., Gómez, E. T. & Jordán, M. M., 2019. Typological characterization of mineral and combustion airborne particles indoors in primary schools. *Atmosphere*, 10(4), 209.

38. Parzych, A., and Sobisz, Z., 2012. The macro-and microelemental content of Pinus sylvestris L. and Pinus nigra JF Arn. needles in Cladonio-Pinetum habitat of the Słowiński National Park.

39. Pasqualini, V., Robles, C., Garzino, S., Greff, S., Bousquet-Mélou, A., & Bonin, G., 2003. Phenolic compounds content in Pinus halepensis Mill. needles: a bioindicator of air pollution. *Chemosphere*, 52(1), 239-248.

40. Pautov, A., Bauer, S., Ivanova, O., Krylova, E., Sapach, Y., Gussarova, G., 2017. Role of the outer stomatal ledges in the mechanics of guard cell movements. *Trees*, 31(1), 125-135.

41. Petrova, S. T., 2020. Efficiency of Pinus nigra JF Arnold in removing pollutants from urban environment (Plovdiv, Bulgaria). *Environmental Science and Pollution Research*, *27*(31), 39490-39506.

42. Petrova, S., 2024. The Added Value of Urban Trees (Tilia tomentosa Moench, Fraxinus excelsior L. and Pinus nigra JF Arnold) in Terms of Air Pollutant Removal. *Forests*, *15*(6), p.1034.

43. Rai, P. K., 2013. Environmental magnetic studies of particulates with special reference to biomagnetic monitoring using roadside plant leaves. *Atmospheric Environment*, *72*, 113-129.

44. Samet, J.M., 2007. Traffic, air pollution, and health. *Inhalation Toxicology*, 19(12), 1021-1027.

45. Sierra-Vargas, M.P., Montero-Vargas, J.M., Debray-García, Y., Vizuet-de-Rueda, J.C., Loaeza-Román, A., Terán, L.M., 2023. Oxidative Stress and Air Pollution: Its Impact on Chronic Respiratory Diseases. *International Journal of Molecular Sciences*, 24 (1), 853.

46. Ștefănuț, S., Manole, A., Ion, C.M, Öllerer, K.Á, Onete, M., Manu, M., Vicol, I., Moldoveanu M.M., Maican S., Banciu C., Cobzaru I., Nicoară R.G., Florescu L.I., Mogîldea, E.D., Purice, D.-M., Nicolae, C.D., Catană, R.D., Văleanu, V.F., Constantin, M., 2017. Ghid de utilizare a speciilor în programele de biomonitorizare. *(https://www.ibiol.ro/biomonro/pdf/ghid/ghidbiomonitorizare.pdf* - accesat la 8.05.2020)

47. Thawale, P.R., Satheesh Babu, S., Wakode, R.R., Singh, S.K., Kumar, S., Juwarkar, A.A., 2011. Biochemical changes in plant leaves as a biomarker of pollution due to anthropogenic activity. *Environmental monitoring and assessment*, *177*, pp.527-535.

48. Valavanidis, A., Fiotakis, K., Vlachogianni, T., 2008. Airborne particulate matter and human health: toxicological assessment and importance of size and composition of

particles for oxidative damage and carcinogenic mechanisms. *Journal of Environmental Sciences and Health*, Part C., 26 (4), 339-362.

49. Wang, X., Wang, Y., Bai, Y., Wang, P. & Zhao, Y., 2019. An overview of physical and chemical features of diesel exhaust particles. *Journal of the Energy Institute*, 92(6), 1864-1888.

50. Wu, L., Luo, X. S., Li, H., Cang, L., Yang, J., Yang, J., Yang, J., Zhao, Z., Tang, M., 2019. Seasonal levels, sources, and health risks of heavy metals in atmospheric PM2. 5 from four functional areas of Nanjing city, eastern China. *Atmosphere 10*(7), 419.

51. Yang, J. B., Yun, H. J., Yeon, M. J., Jeoung, D., Jo, K. N., Jung, H. S., 2020. Electron microscopic and spectroscopic analysis of airborne ultrafine particles: its effects on the cell viability. *Journal of Analytical Sciences and Technology*, 11, 1-8.

52. Zeiner, M., Juranović Cindrić, I., 2021. Accumulation of major, minor and trace elements in pine needles (Pinus nigra) in Vienna (Austria). *Molecules*, *26*(11), p.3318.

53. Zhang, R., Wang, G., Guo, S., Zamora, M. L., Ying, Q., Lin, Y., Wang, W., Hu, M, Wang, Y., 2015. Formation of urban fine particulate matter. *Chemical reviews*, 115(10), 3803-3855.

54. Zsigmond, A. R., Száraz, A., & Urák, I., 2021. Macro and trace elements in the black pine needles as inorganic indicators of urban traffic emissions. *Environmental Pollution*, *291*, 118228.